Imaging the structure of atomic nuclei with high energy nuclear collisions

Chunjian Zhang

RIKEN BNL Research Center (RBRC), Feb. 08, 2024

Stony Brook University

Outline

1. Nuclear structure connection to heavy-ion collisions

2. Nuclear deformation in ^{238}U nucleus

3. Nuclear structure in isobaric ^{96}Ru and ^{96}Zr nuclei

4. Nucleonic clustering in ^{16}O light nucleus

5. Conclusions and outlooks

Section 1: Nuclear structure connection to heavy-ion collisions

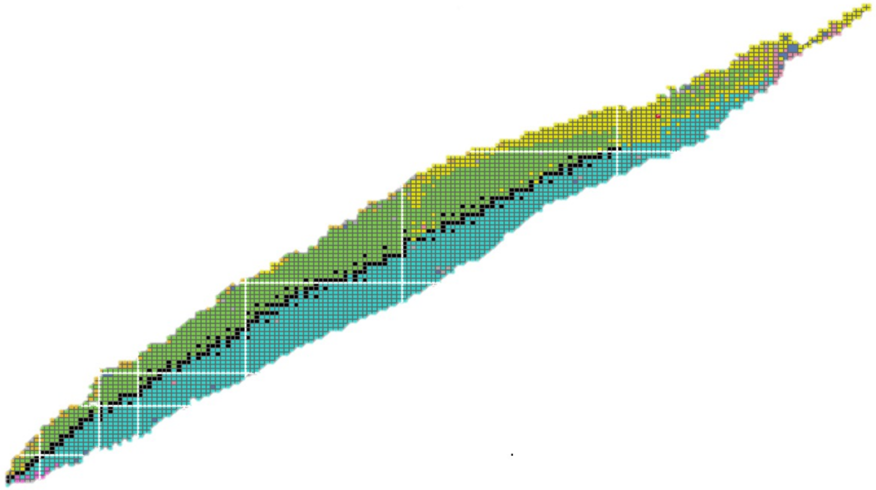

Nuclear deformation
Neutron skin
Nucleonic clustering
….

?

Low energy community

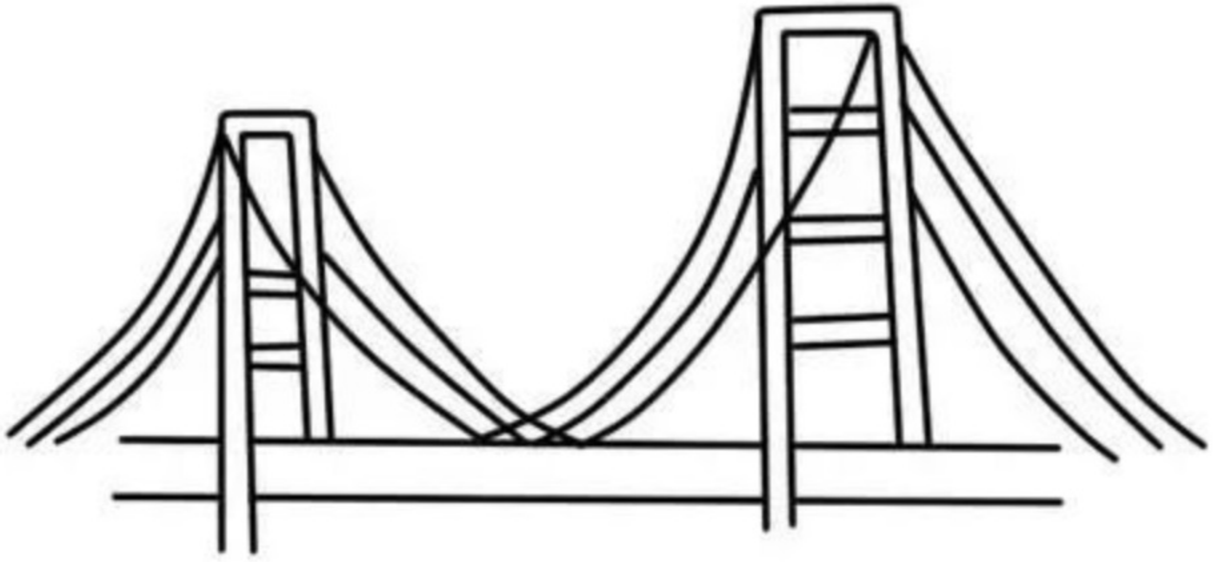

Heavy-ion community

Recap the moments for understanding the nuclear structure

Rutherford model

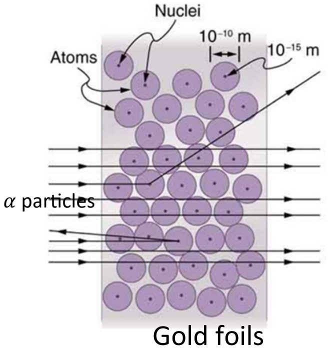

Rutherford, 1911

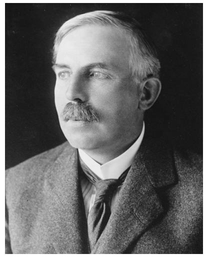

Fermi-Gas model

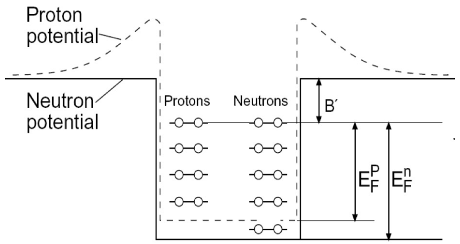

Fermi, 1932

Liquid drop model

George, Bohr and John, 1936



Shell model

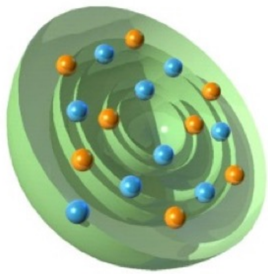

Mayer and Jensen, 1949


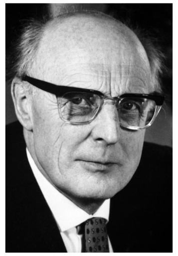

 1963

Collective model

Bohr and Mottelson, 1953


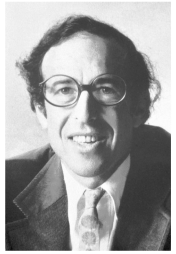

 1975

Density-functional theory

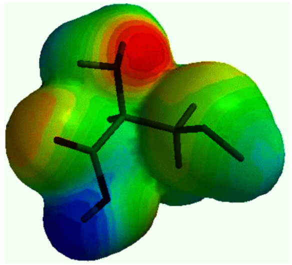

Walter Kohn,1964

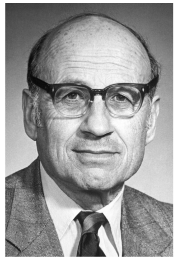

1/2  1998

https://www.nobelprize.org/prizes/lists/all-nobel-prizes-in-physics/

Collective structure of atomic nuclei

- Emergent phenomena of the many-body quantum system
  - Quadrupole/octupole/hexadecapole deformations
  - Clustering, halo, skin, bubble…
  - Non-monotonic evaluation with N and Z

RepProgPhys76, 126301(2013)

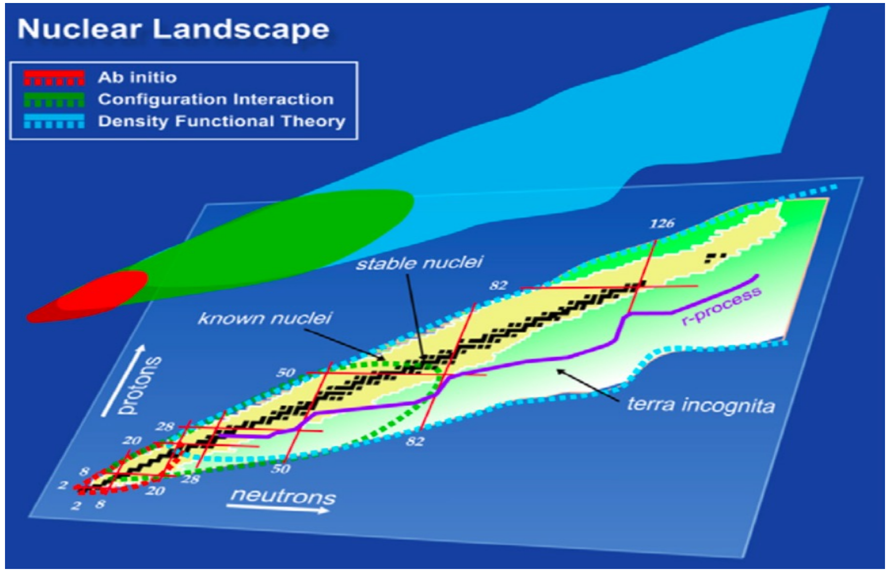

Quadrupole

S. Cwiok et al.,Nature433, 705(2005)

Octupole

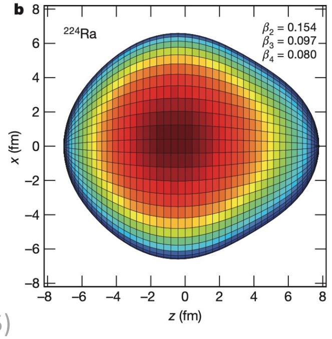

LP Gaffney et al., Nature497, 199(2013)

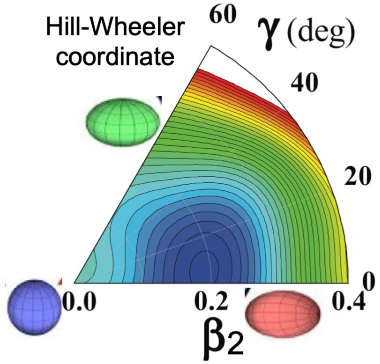

Triaxial spheroid

AN Andreyev et al., Nature405, 430(2000)

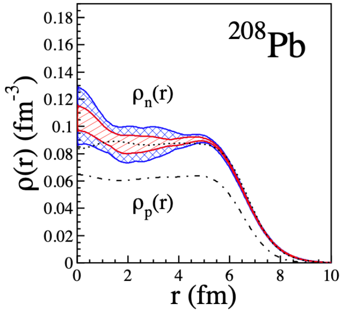

Neutron skin

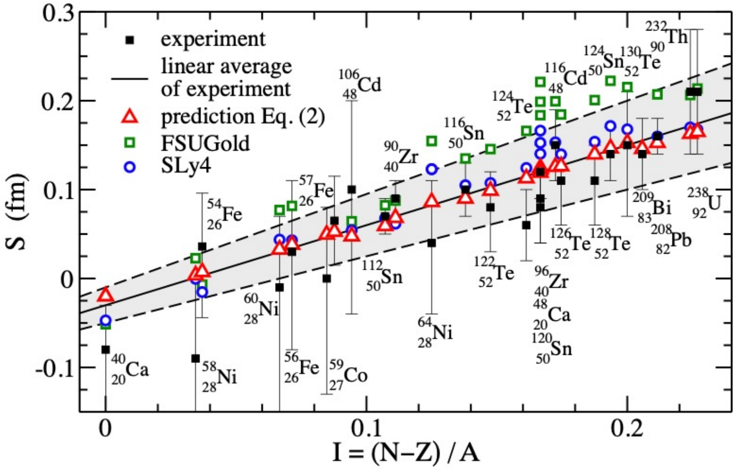

A. Trzcinska et al., PRL87, 082501(2001)
B. M. Centelles et al., PRL102, 122502(2009)

nucleonic clustering

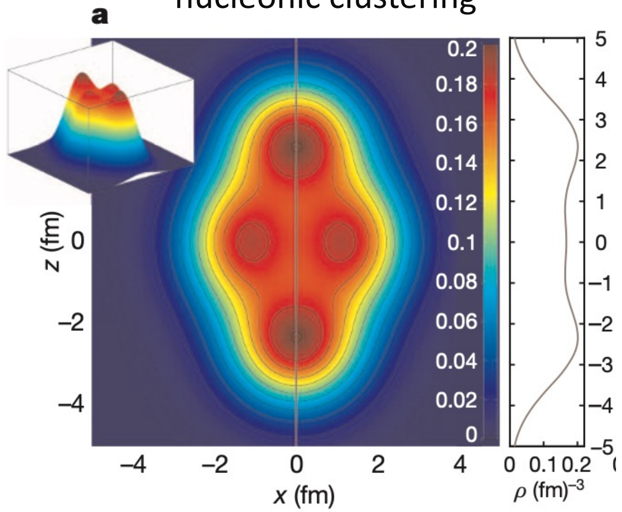

J.P. Ebran et al. Nature487, 341(2012)

Multi-stages in relativistic heavy-ion collisions

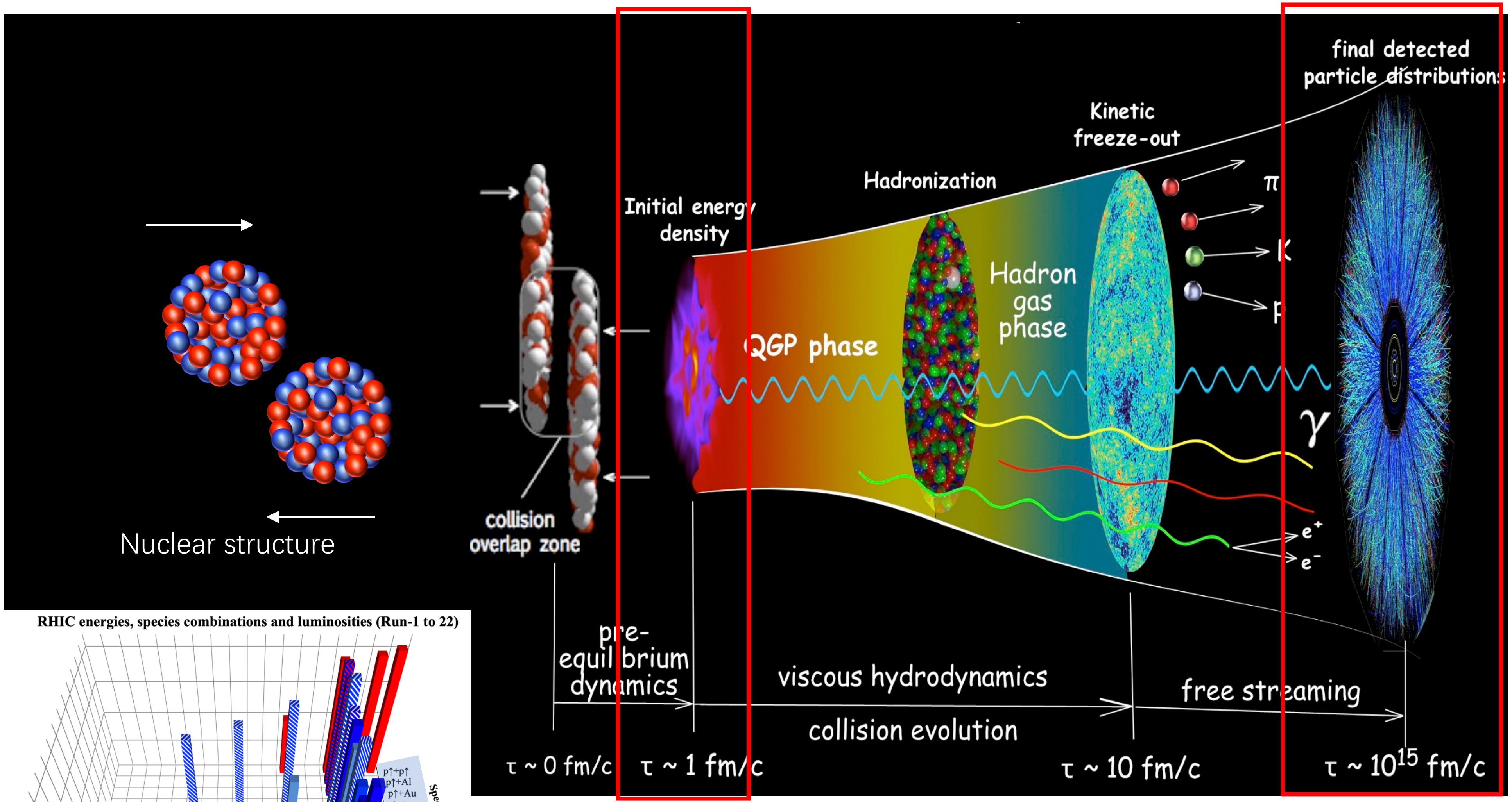

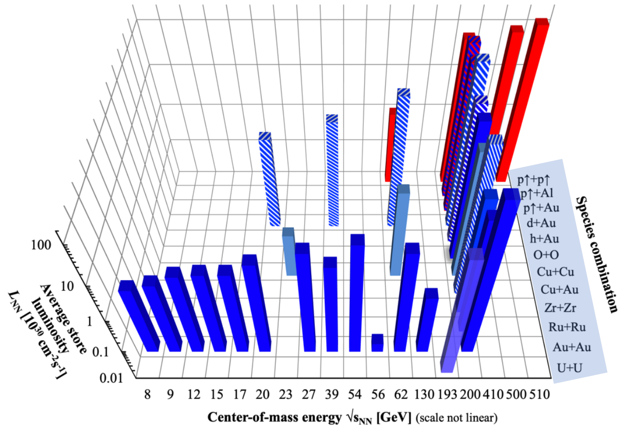

$$e(x,y) \sim \begin{cases} T_A + T_B & N_{\rm part}-\text{scaling}, p=1 \\ T_A T_B & N_{\rm coll}-\text{scaling}, p=0, q=2 \\ \sqrt{T_A T_B} & \text{Trento default}, p=0 \\ \min\{T_A, T_B\} & \text{KLN model}, p\sim -2/3 \\ T_A + T_B + \alpha T_A T_B & \text{two-component model,} \\ & \text{similar to quark-glauber model} \end{cases}$$

$$T \propto \left(\frac{T_A^p + T_B^p}{2}\right)^{q/p}$$

Multiple stage
/Complex dynamics

Hybrid multi-stage
Modeling with event-by
-event fluctuations

Collective flow assisted nuclear structure imaging

Nuclear structure

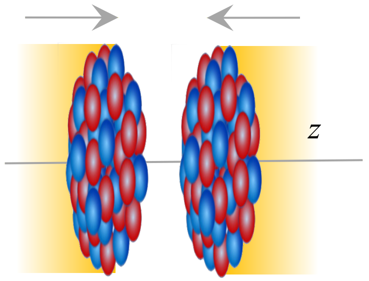

Imaging

$$\rho(r,\theta,\phi) = \frac{\rho_0}{1+e^{(r-R(\theta,\phi))/a_0}}$$

$$R(\theta,\phi) = R_0(1+\beta_2[\cos\gamma Y_{2,0}(\theta,\phi)+\sin\gamma Y_{2,2}(\theta,\phi)]+\beta_3 Y_{3,0}(\theta,\phi))$$

- β_2 → Quadrupole deformation
- β_3 → Octupole deformation
- γ → Triaxiality
- a_0 → Surface diffuseness
- R_0 → Nuclear size

?

Initial state

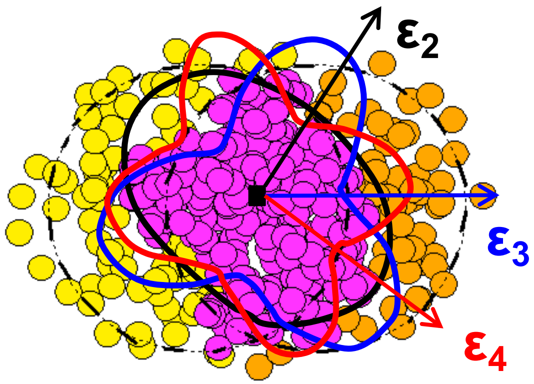

$$F = -\nabla P(\epsilon)$$

hydro-response

Final state

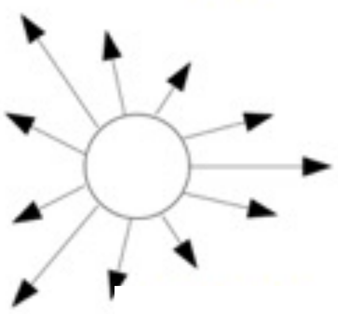

Initial Size

$$R_\perp^2 \propto \langle r_\perp^2 \rangle$$

Initial Shape

$$\mathcal{E}_n \propto \langle r_\perp^n e^{in\phi} \rangle$$

R_0 a_0 β_n

Radial Flow

Anisotropic Flow

$$\frac{d^2N}{d\phi dp_T} = N(p_T)\left(\sum_n V_n e^{-in\phi}\right)$$

$$N_{ch} \propto N_{part} \quad \frac{\delta[p_T]}{[p_T]} \propto -\frac{\delta R_\perp}{R_\perp} \quad V_n \propto \mathcal{E}_n$$

High energy: Large multiplicity and boost invariance; approximate linear response in each event

- Constrain the initial condition by comparing nuclei with known structure properties.
- Reveal novel properties of nuclei by leveraging known hydrodynamic response.
- Study the unknown nuclear structure by heavy-ion collisions.

Connecting the initial conditions to the nuclear shape

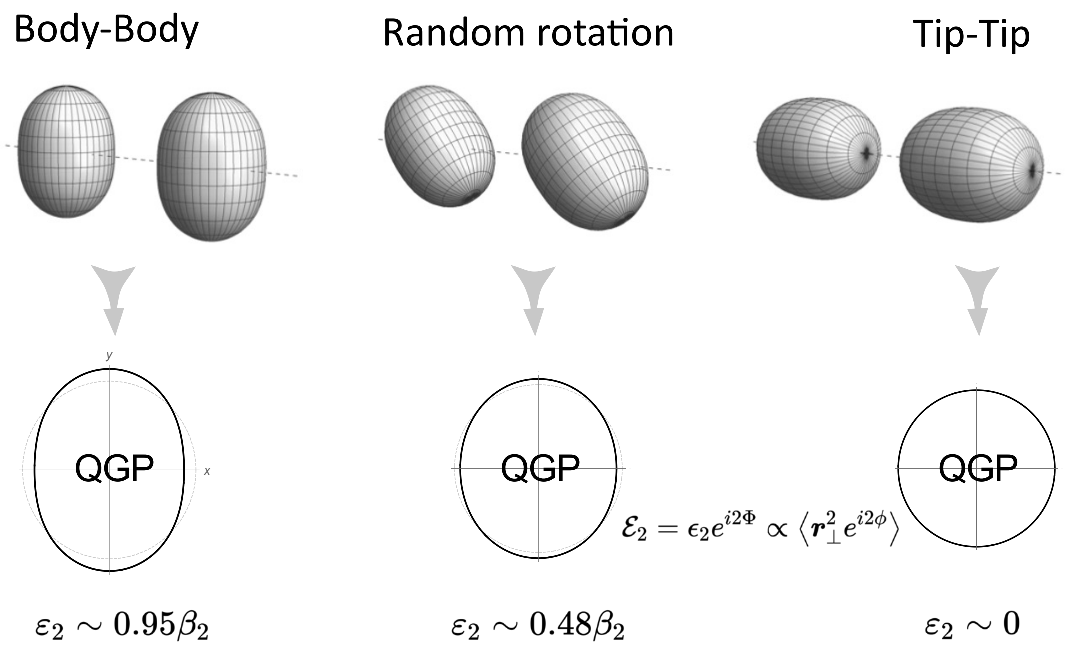

$$\boldsymbol{\epsilon}_2 = \underbrace{\boldsymbol{\epsilon}_0}_{\text{undeformed}} + \underbrace{\boldsymbol{p}(\Omega_1, \Omega_2)}_{\text{phase factor}}\beta_2 + \mathcal{O}(\beta_2^2)$$

$$\langle \epsilon_2^2 \rangle \approx \langle \epsilon_0^2 \rangle + 0.2\beta_2^2$$

$$\langle v_n^2 \rangle \propto \langle \epsilon_n^2 \rangle$$

Shape depends on Euler angle Ω=ϕθψ

J. Jia, PRC105, 014905(2022)

$$\rho(r,\theta,\phi) = \frac{\rho_0}{1 + e^{(r - R(\theta,\phi))/a_0}}$$

$$R(\theta,\phi) = R_0(1 + \beta_2[\cos\gamma Y_{2,0}(\theta,\phi) + \sin\gamma Y_{2,2}(\theta,\phi)] + \beta_3 Y_{3,0}(\theta,\phi))$$

- In principle, can measure any moments of $p(1/R, \varepsilon_2, \varepsilon_3\ldots)$
  - Mean $\langle d_\perp \rangle$
  - Variance $\langle \varepsilon_n^2 \rangle$, $\left\langle (\delta d_\perp/d_\perp)^2 \right\rangle$
  - Skewness $\langle \varepsilon_n^2 \delta d_\perp/d_\perp \rangle$, $\left\langle (\delta d_\perp/d_\perp)^3 \right\rangle$
  - Kurtosis $\langle \varepsilon_n^4 \rangle - 2\langle \varepsilon_n^2 \rangle^2$, $\left\langle (\delta d_\perp/d_\perp)^4 \right\rangle - 3\left\langle (\delta d_\perp/d_\perp)^2 \right\rangle^2$
- All have a simple connection to deformation
  - Two-points correlation
  - Three-points correlation

$$\langle \varepsilon_2^2 \rangle \sim a_2 + b_{2,2}\langle \beta_2^2 \rangle + b_{2,3}\langle \beta_3^2 \rangle$$
$$\langle \varepsilon_3^2 \rangle \sim a_3 + b_{3,3}\langle \beta_3^2 \rangle + b_{3,4}\langle \beta_4^2 \rangle$$
$$\langle \varepsilon_4^2 \rangle \sim a_4 + b_{4,4}\langle \beta_4^2 \rangle$$
$$\left\langle (\delta d_\perp/d_\perp)^2 \right\rangle \sim a_0 + b_0\beta_2^2 + b_{0,3}\beta_3^2$$

$$\langle \varepsilon_2^2 \delta d_\perp/d_\perp \rangle \sim a_1 - b_1 \cos(3\gamma)\beta_2^3$$
$$\left\langle (\delta d_\perp/d_\perp)^3 \right\rangle \sim a_2 - b_2 \cos(3\gamma)\beta_2^3$$

Low-energy spectroscopy vs high-energy snapshot method

- Intrinsic frame shape not directly visible in lab frame at time scale

STAR, arXiv:2401.06625v1

--Mainly inferred from non-invasive spectroscopy methods.

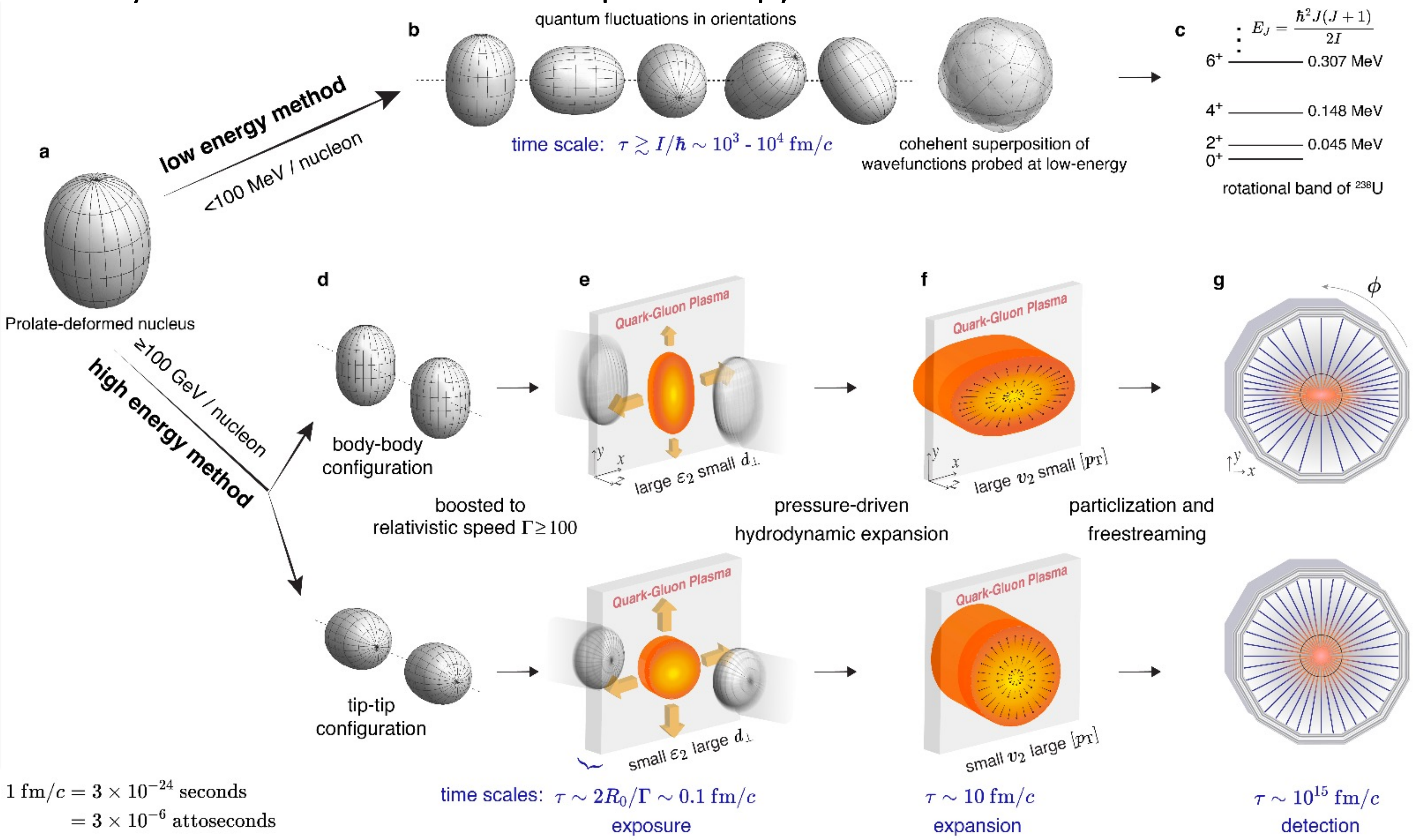

- Shape-frozen like snapshot in nuclear crossing (10^{-25}s << rotational time scale 10^{-21}s)

--probe entire mass distribution in the intrinsic frame via multi-point correlations.

Section 2: Nuclear deformation in ^{238}U

$$\rho(r,\theta,\phi) = \frac{\rho_0}{1+e^{(r-R(\theta,\phi))/a_0}}$$

$$R(\theta,\phi) = R_0(1+\beta_2[\cos\gamma Y_{2,0}(\theta,\phi)+\sin\gamma Y_{2,2}(\theta,\phi)]+\beta_3 Y_{3,0}(\theta,\phi)+\beta_4 Y_{4,0}(\theta,\phi))$$

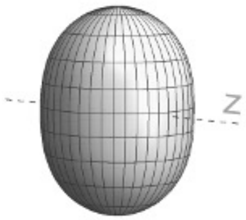

W. Ryssens et al., PRL130, 212302(2023)

DFT calculations predict a smaller WS deformation $\beta_{2\mathrm{U}} \approx 0.28 \rightarrow \beta_{2\mathrm{U,WS}} \approx 0.25$

corresponding to a larger volume deformation in presence of $\boldsymbol{\beta}_{4\mathrm{U}}$~0.1 $\beta_{2,\mathrm{body}} = \frac{4\pi}{3R_0^2 A}\int d^3r\rho(\mathbf{r})r^2 Y_{20}$

Low-energy estimate with rigid rotor assumption from B(E2) data $\beta_{2,\mathrm{LD}} = \frac{4\pi}{5R_0^2 Z}\sqrt{\frac{B(\mathrm{E2})}{e^2}}$

$\beta_{2\mathrm{U,LD}} = 0.287 \pm 0.007 \quad \gamma_{\mathrm{U,LD}} = 6^\circ - 8^\circ$

B. Pritychenko et al., J.ADT.107, 1(2016)
C. Y. Wu et al., PRC54, 2356(1996)

Evidence of deformation from system comparison

Enhancement v_{2U}/v_{2Au} is the effect from deformation

Also see, STAR, PRL115, 222301(2015)

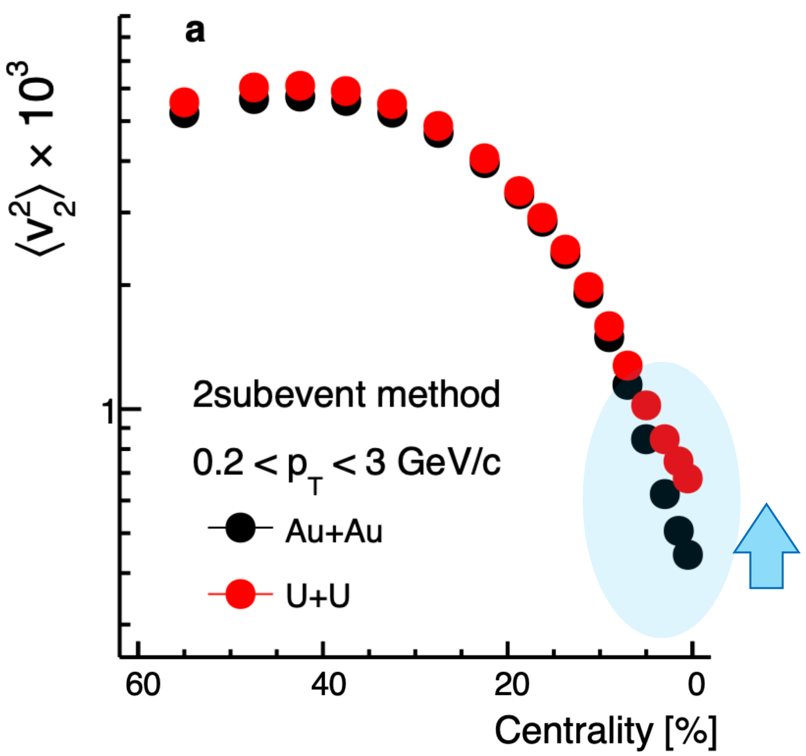

Confirm the role of β_2

Final state implemented in AMPT transport model

G. Giacalone, J. Jia, and C.Zhang, PRL127, 242301(2021)

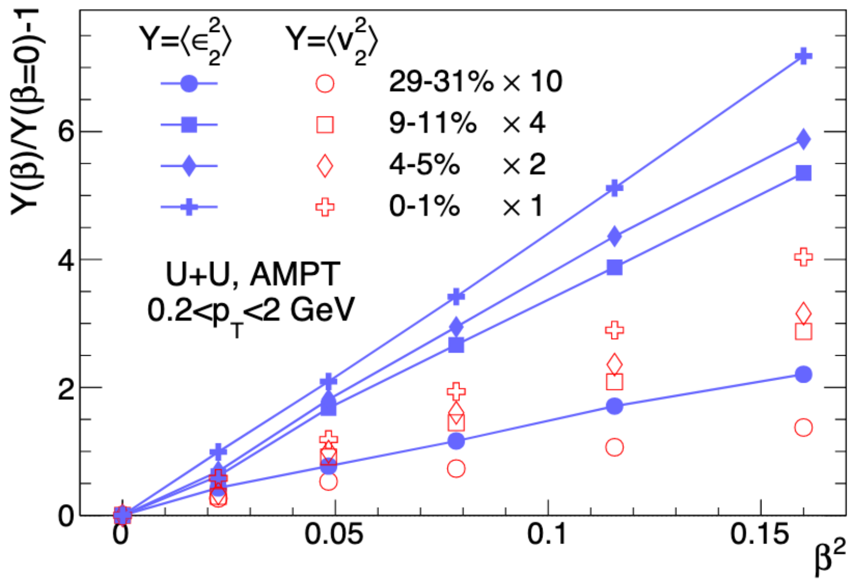

$$\langle v_2^2 \rangle \approx a + b\langle \beta_2^2 \rangle$$

- a strict linear relation has been observed
- Reliable extraction for deformation in the UCC region

Mean transverse momentum $[p_T]$ fluctuations

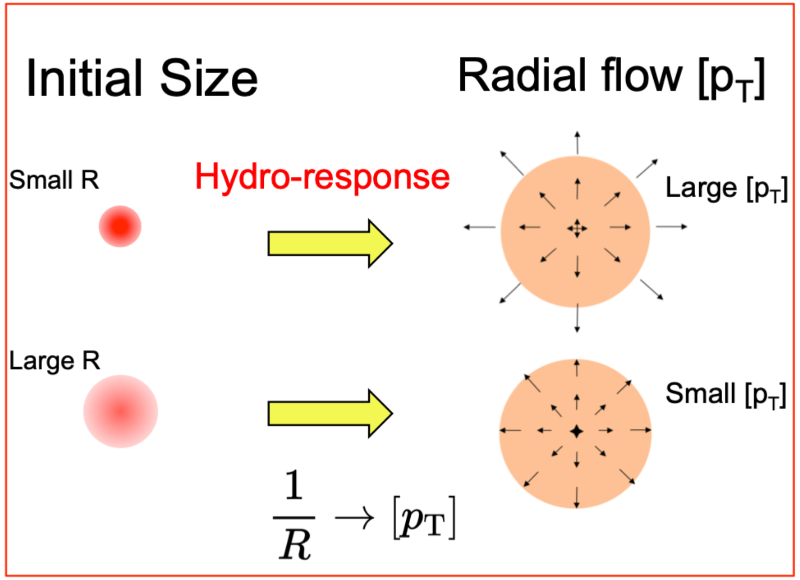

J.Jia, PRC105, 044905(2022)

Mean $\frac{\delta[p_T]}{[p_T]} \propto \frac{\delta d_\perp}{d_\perp} \propto \beta_2$

Variance $\left\langle \left(\frac{\delta[p_T]}{[p_T]}\right)^2 \right\rangle \propto \left\langle \left(\frac{\delta d_\perp}{d_\perp}\right)^2 \right\rangle \propto \beta_2^2$

Skewness $\left\langle \left(\frac{\delta[p_T]}{[p_T]}\right)^3 \right\rangle \propto \left\langle \left(\frac{\delta d_\perp}{d_\perp}\right)^3 \right\rangle \propto cos(3\gamma)\beta_2^3$

Kurtosis $\left\langle \left(\frac{\delta[p_T]}{[p_T]}\right)^4 \right\rangle - 3\left\langle \left(\frac{\delta[p_T]}{[p_T]}\right)^2 \right\rangle^2 \propto \left\langle \left(\frac{\delta d_\perp}{d_\perp}\right)^4 \right\rangle - 3\left\langle \left(\frac{\delta d_\perp}{d_\perp}\right)^2 \right\rangle^2 \propto -\beta_2^4$

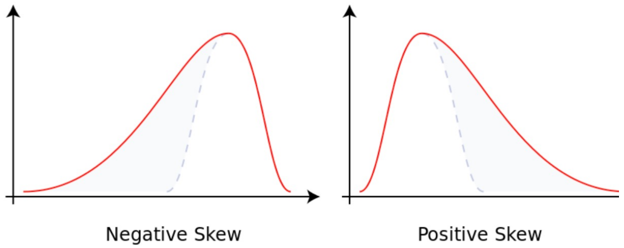

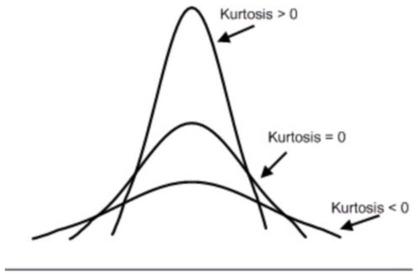

Variance

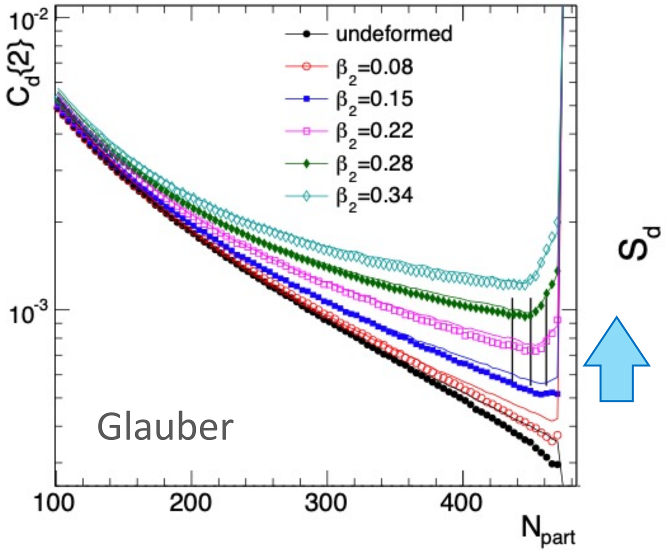

Skewness

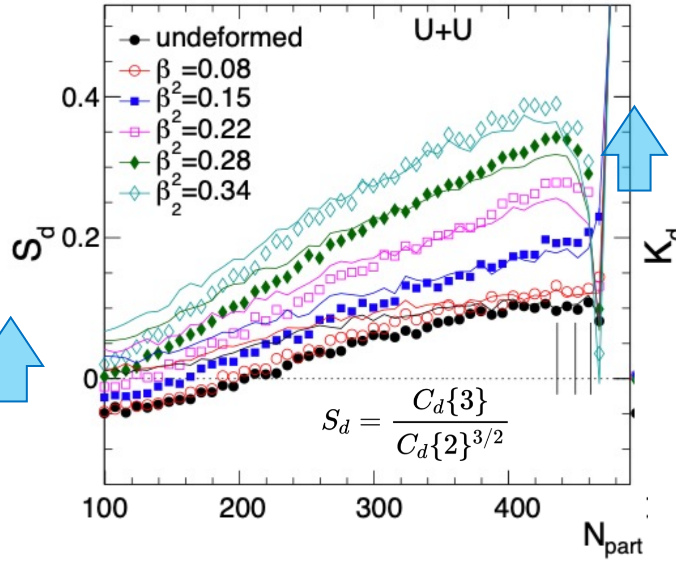

Kurtosis

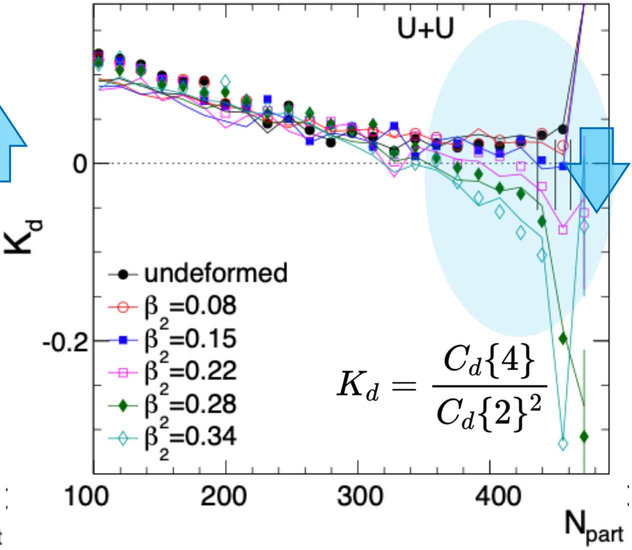

S. Bhatta, C. Zhang and J. Jia, PRC105, 024904(2022)

Event-by-event fluctuations also reflect the deformation of colliding nuclei

$[p_T]$ fluctuations and comparisons to hydro model

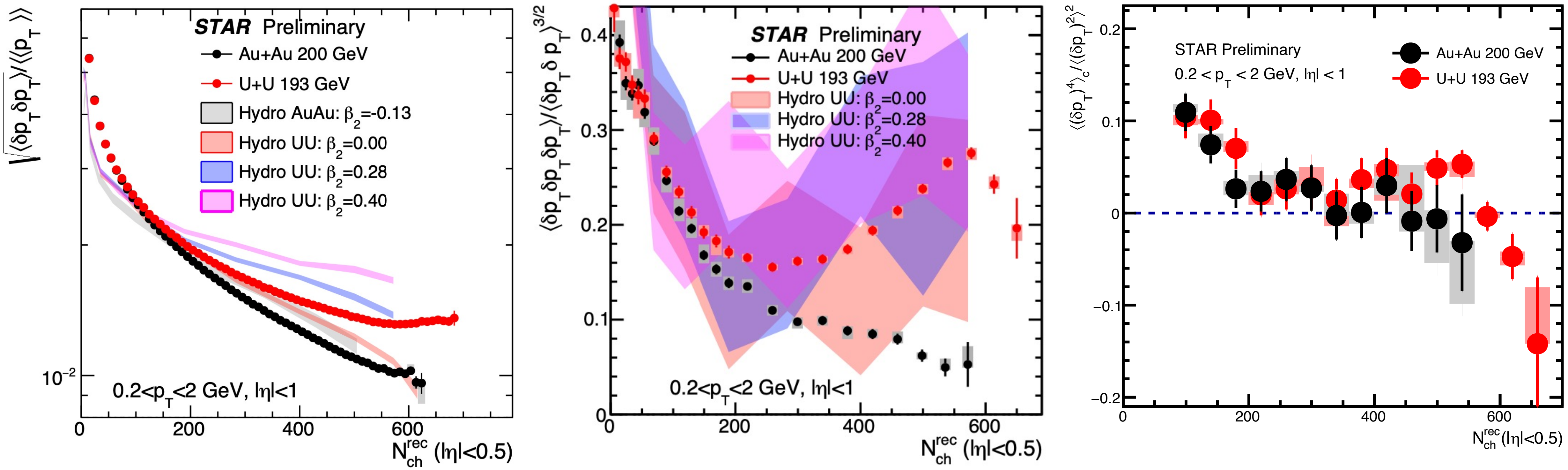

Au+Au: variance and skewness follow independent source scaling $1/N_s^{n-1}$ within power-law decrease

U+U: large enhancement in normalized variance and skewness and sign-change in normalized kurtosis

⟶ size fluctuations enhanced

The nuclear deformation role is further confirmed by hydro calculations.

Hydro: private calculations are provided by Bjoern Schenke and Chun Shen

$[p_T]$ fluctuations also serve as a good observable to explore the role of nuclear deformation.

Reflecting the initial state from the nuclear geometry

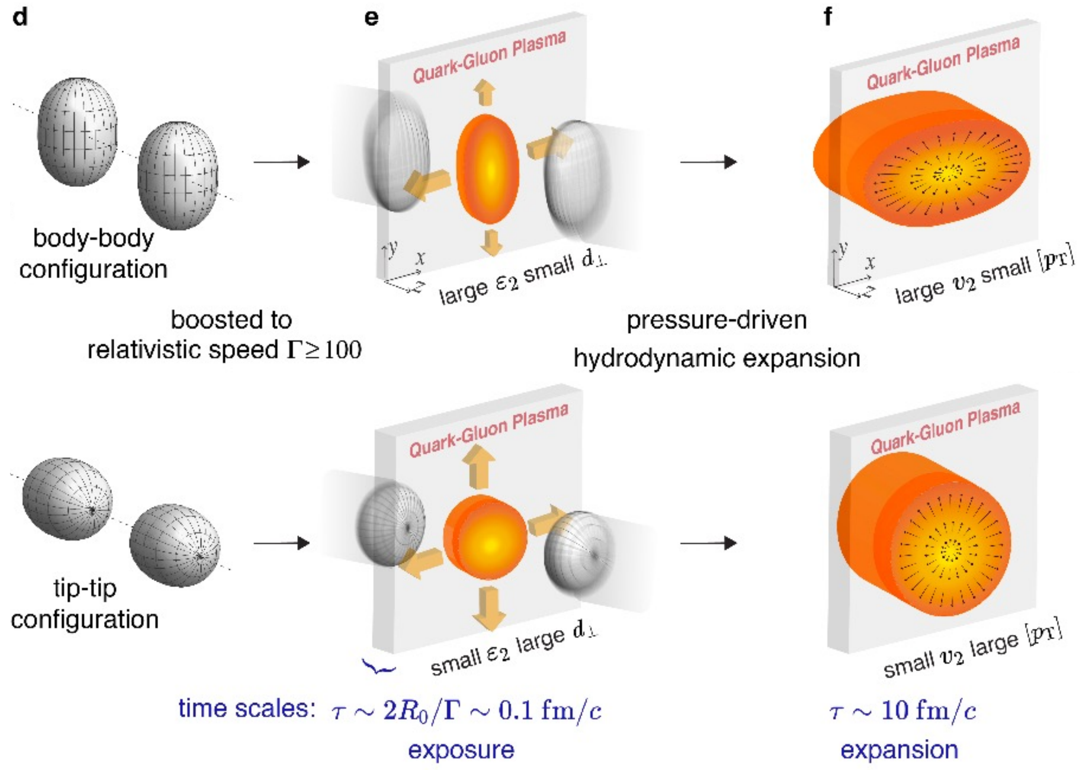

STAR, arXiv:2401.06625v1

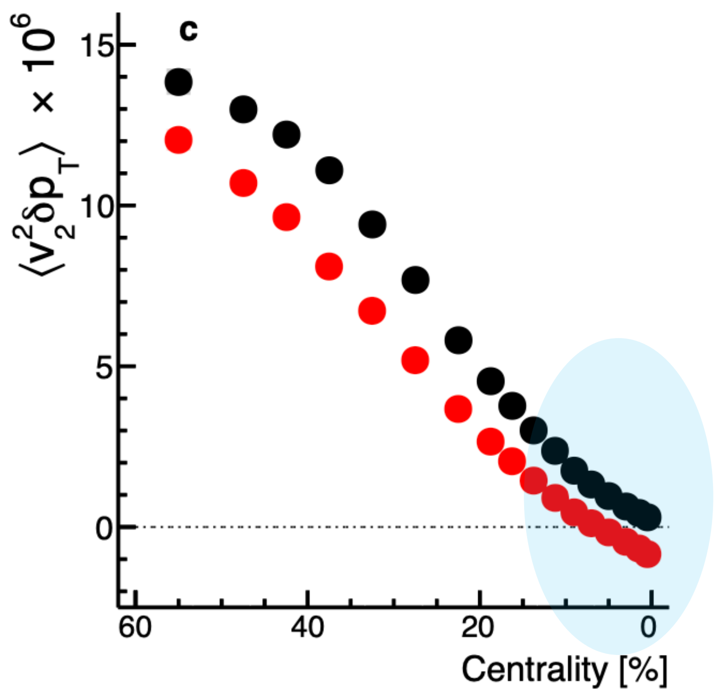

v_n-$[p_T]$ three particle correlator

$$\mathrm{cov}\left(v_n^2, [p_T]\right) \equiv \left\langle \frac{\sum_{i\neq j\neq k} w_i w_j w_k e^{in\phi_i} e^{-in\phi_j}\left(p_{T,k} - \langle\langle p_T\rangle\rangle\right)}{\sum_{i\neq j\neq k} w_i w_j w_k} \right\rangle_{\mathrm{evt}}$$

$$[p_T] \equiv \frac{\sum_i w_i p_{T,i}}{\sum_i w_i}, \langle\langle p_T\rangle\rangle \equiv \langle [p_T]\rangle_{\mathrm{evt}}$$

w_i is track weight

- $\boldsymbol{\varepsilon}_2$ and R are influenced by the quadrupole deformation β_2
- $\langle p_T \rangle \sim 1/R$ and $v_2 \propto \boldsymbol{\varepsilon}_2$: $\left\langle \epsilon_n^2 \frac{1}{R} \right\rangle \rightarrow \left\langle v_n^2\, p_T \right\rangle$

deformation contributes to anticorrelation between v_2 and $\langle p_T \rangle$

P. Bozek, PRC93, 044908(2016)
G Giacalone, PRL124, 202301(2020)
J. Jia, S. Huang and C. Zhang, PRC105, 014906(2022)

Sign-change in U+U in central collisions; Au+Au remains positive

Extracting shape of ^{238}U: quadrupole deformation and triaxiality

STAR, arXiv:2401.06625v1

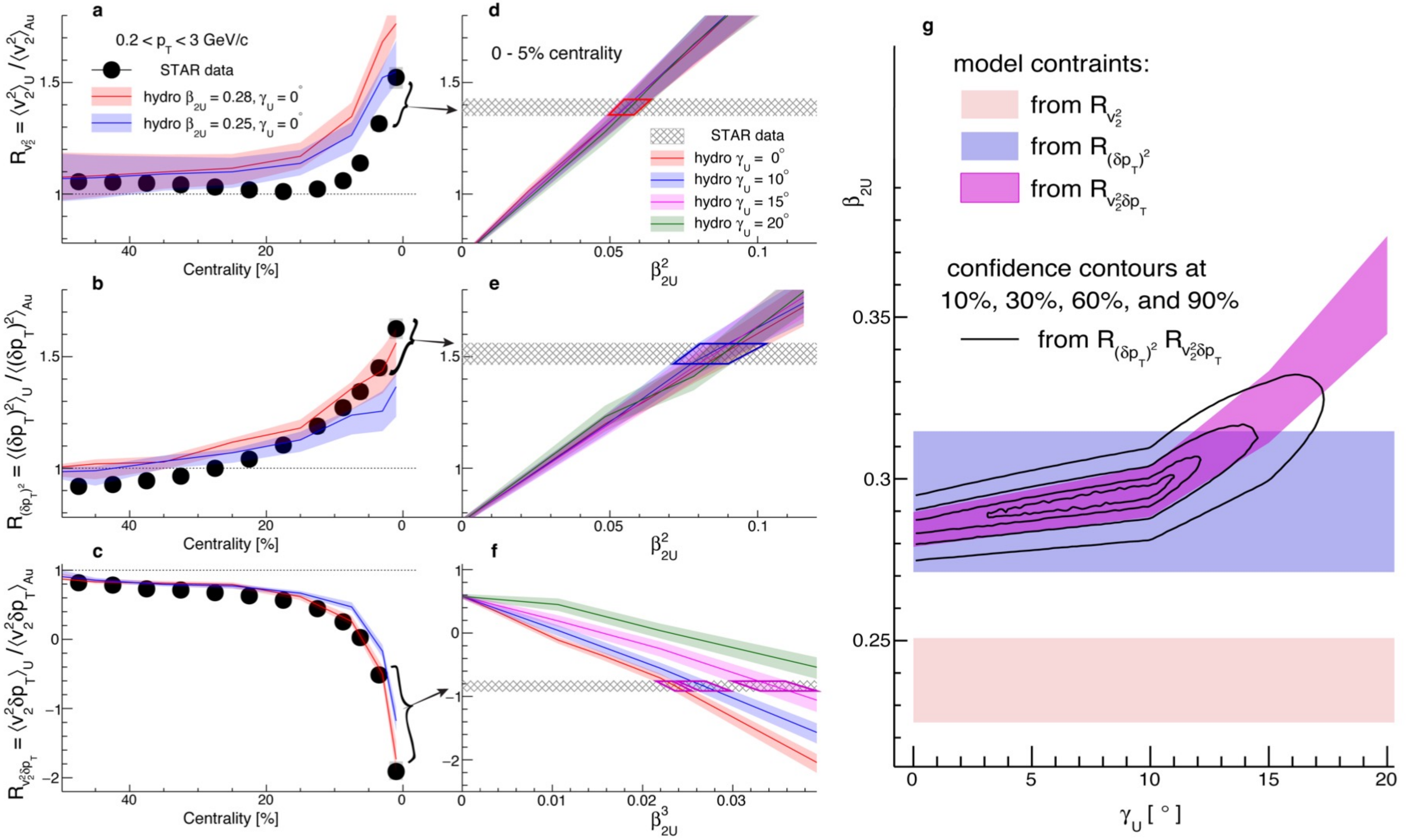

Achieves a better description of ratios in UCC region

$$\langle v_2^2 \rangle = a_1 + b_1 \beta_2^2$$

$$\left\langle (\delta p_{\mathrm{T}})^2 \right\rangle = a_2 + b_2 \beta_2^2$$

$$\langle v_2^2 \delta p_{\mathrm{T}} \rangle = a_3 - b_3 \beta_2^3 \cos(3\gamma)$$

Constraints on β_2 of ^{238}U from data comparison with hydro

$$\beta_{2\mathrm{U}} = 0.297 \pm 0.013$$

$$\gamma_U = 8.6^\circ \pm 4.8^\circ$$

Understanding the nuclear structure in the different time scales.

The heavy-ion collisions could also quantify the shape of ^{238}U as a complementary tool.

Extracting shape of ^{238}U: robust and remarkable in central collisions

Effect from nuclear parameters are smaller and included in systematics

Ratios cancel the viscosity effects.

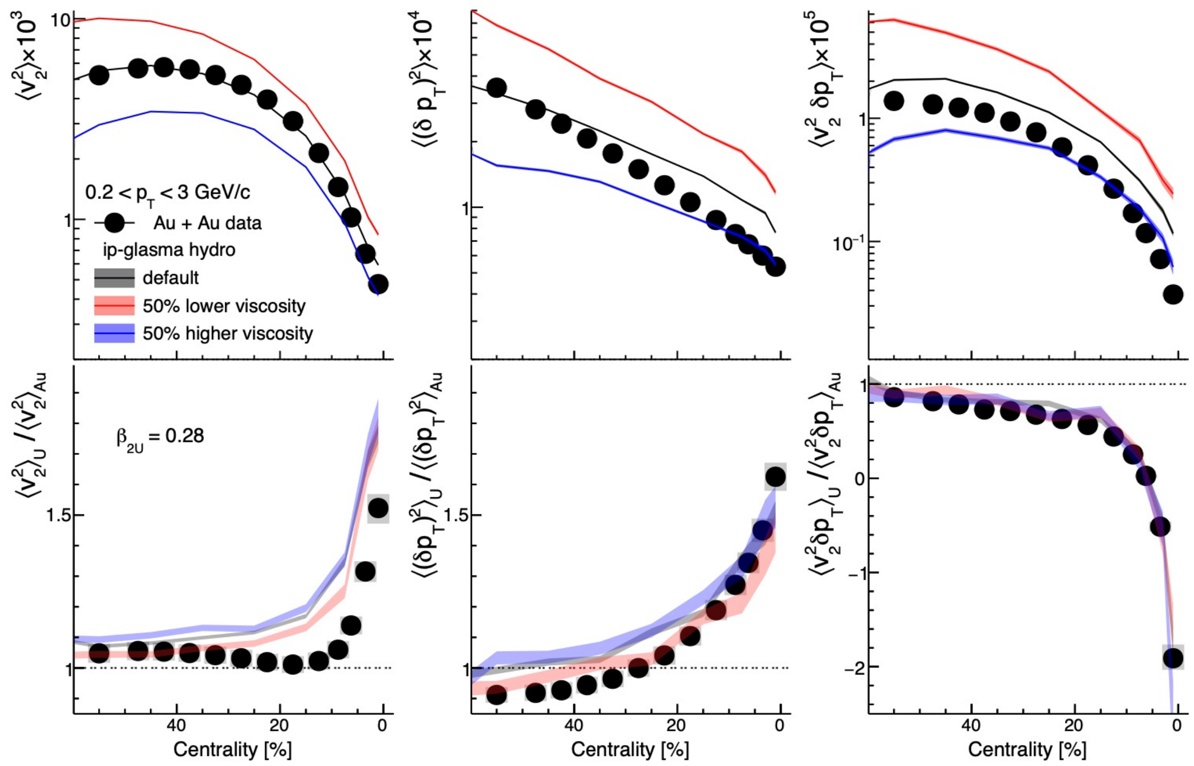

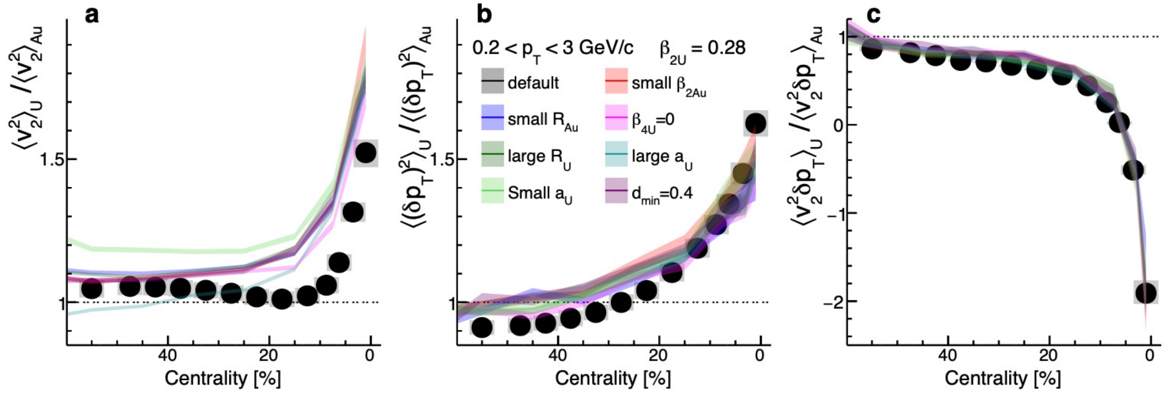

Other hydrodynamics models (Trajectum) also show rather consistent extractions even if it was not tuned to RHIC data.

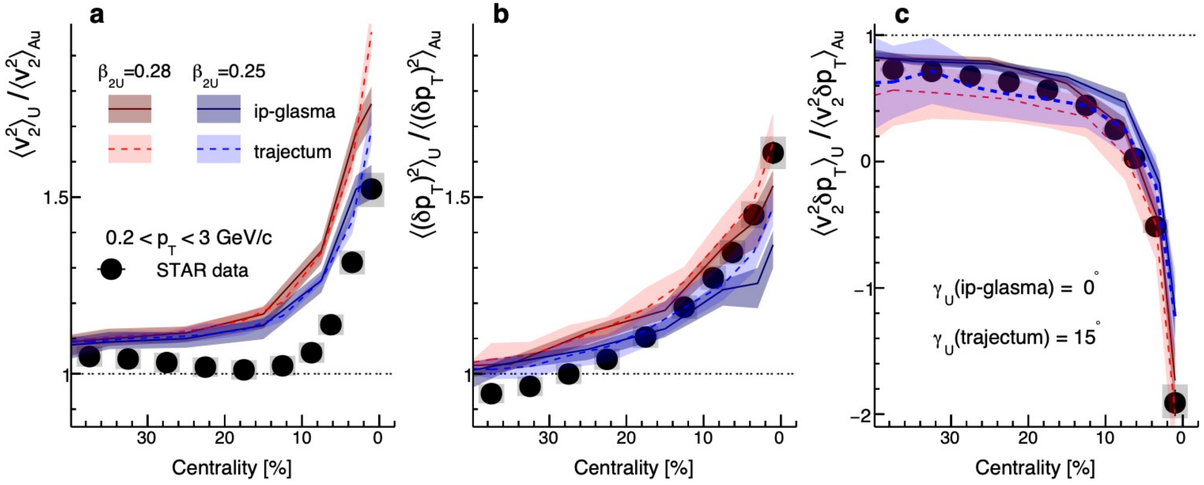

STAR, arXiv:2401.06625v1

Estimate from Scalar Product

Phys. Rev. Lett. 93 (2004) 252301

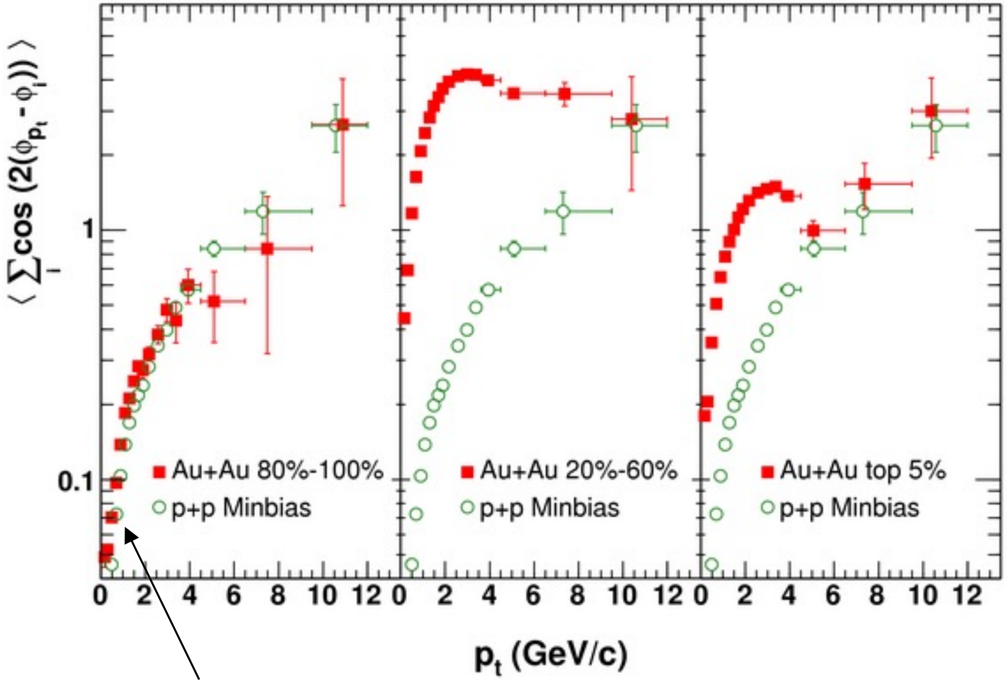

80-100% may has 30% flow estimated by Shengli

Scalar product method or "u**Q**=$v_{22}N_{ch}$" method
Q: 0.15-2.0GeV/c; raw TPC track,
no occupancy correction(~20-30% in central)

Nonflow for integrated uQ: [0.2-2GeV/c]

Ingegrated u**Q** = Σu(pt) Q $*$ Yield(pt)/ΣYield(pt)/

Charge hadron pT spectra: PRL. 91 (2003) 172302

Nonflow(0.2-2GeV/c) for full event(FE) in 0-5% AuAu = 10.2%
Correcting for Occupancy: ~ 8% (standard method), 4% (subevent method)

Consistent with the estimation from 70-80% by assuming 40% nonflow in it.

For FE, HIJING is higher than data. But its non-flow decreases slowly with $\boldsymbol{\Delta\eta}$ compared to data.

Hijing pp vs. Data pp

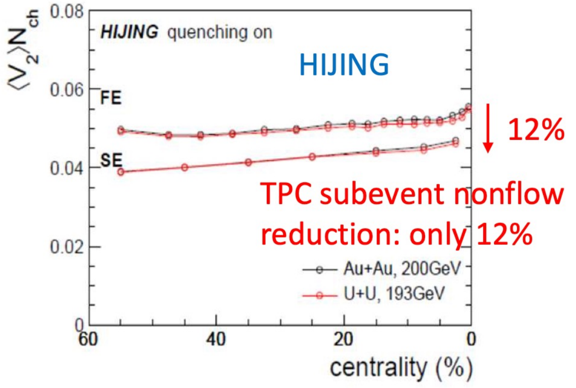

Large away side, fat near-side

HIJING only has 12% reduction for SE.

HIJING pp

Two-particle correlation function

$|\Delta\eta|$>0, 0.2 …. >1.6

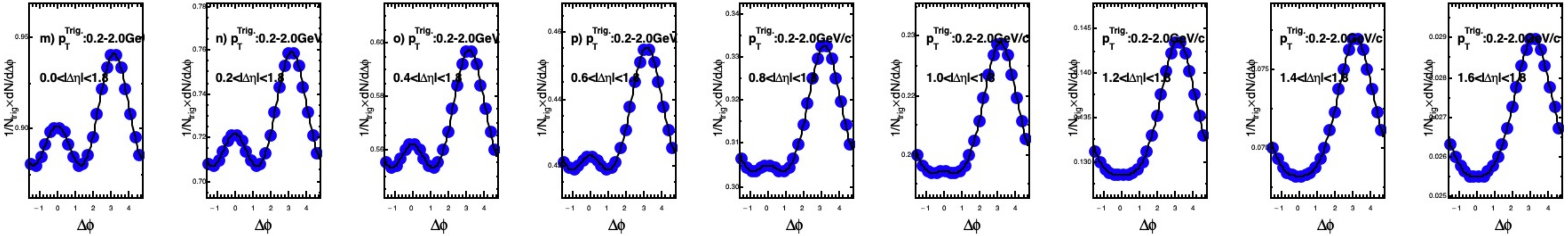

Significantly different from pp data we checked!

HIJING significantly overestimated nonflow in subevent

HIJING pp: SE only remove 12% nonflow, subevent overestimate nonflow
Taking this into account:
u***Q** data method : FE(8%) SE(4%) UU/AuAu ratio will be 4% (FE) and 2% (SE)
HIJING+SE/FE data: FE(12%) SE(6%) UU/AuAu ratio will be 6% (FE) and 3% (SE)

Jet fragmentation and residual contribution to v_2^2

x2 reduction from
subevent in peripheral

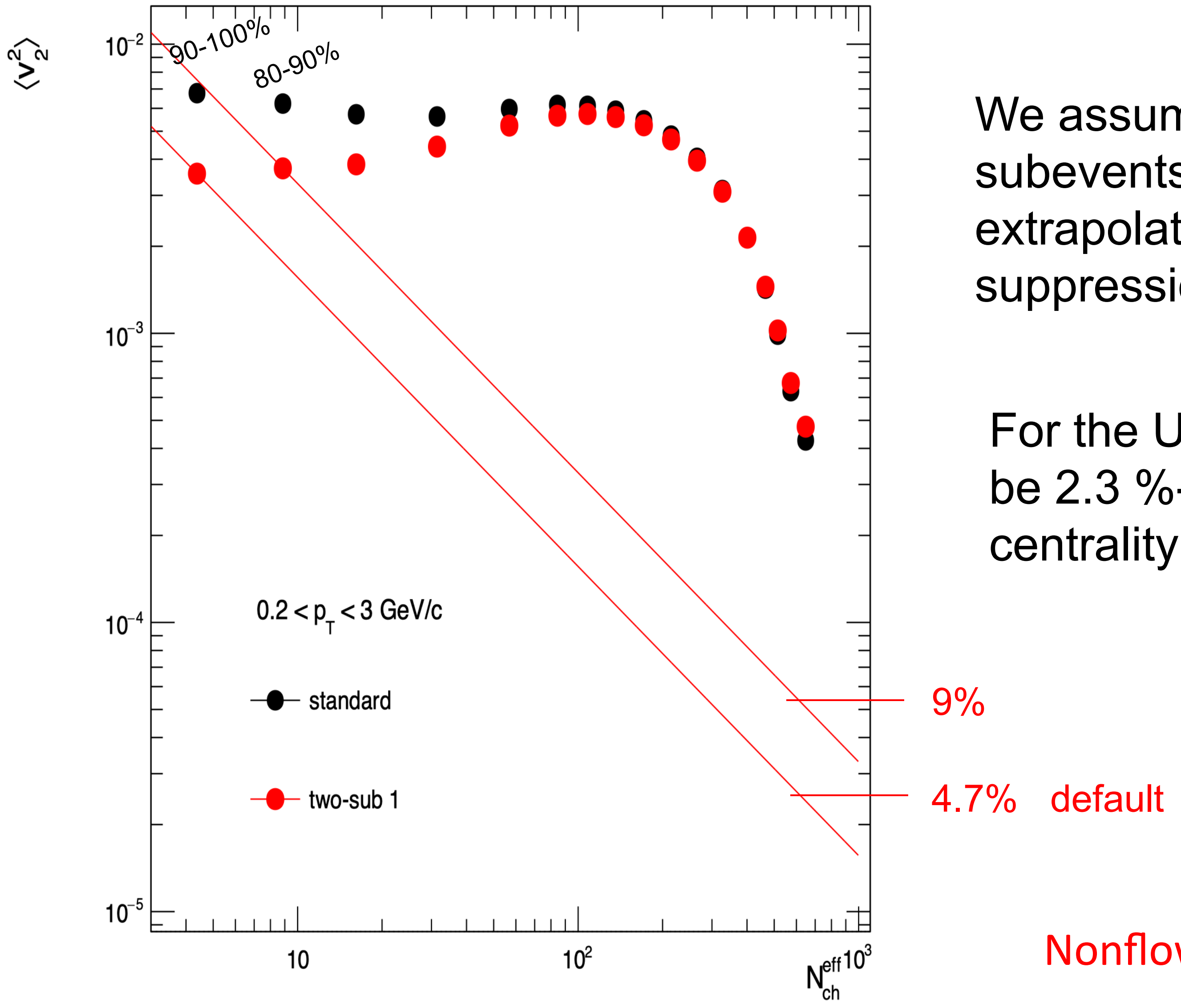

We assume all correlations in subevents are background, and extrapolate assuming no jet suppression (1/N scaling)

For the UU/AuAu ratios it should be 2.3 %- 4.5 % in 0-5% centrality

Nonflow would not affect the conclusions!

v_2^2-p_T correlator

HIJING overestimate the peripheral >60% centrality by a lot.

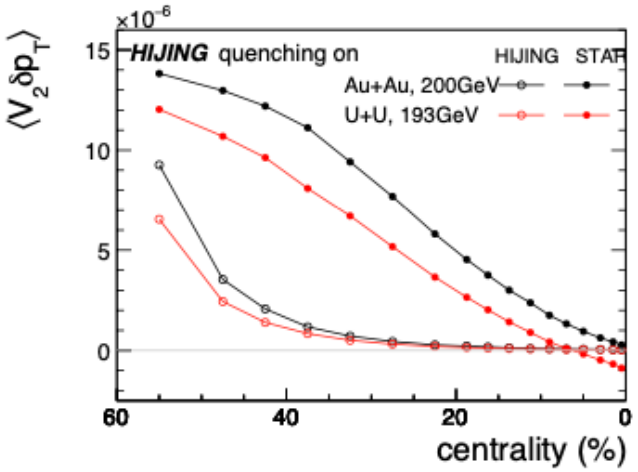

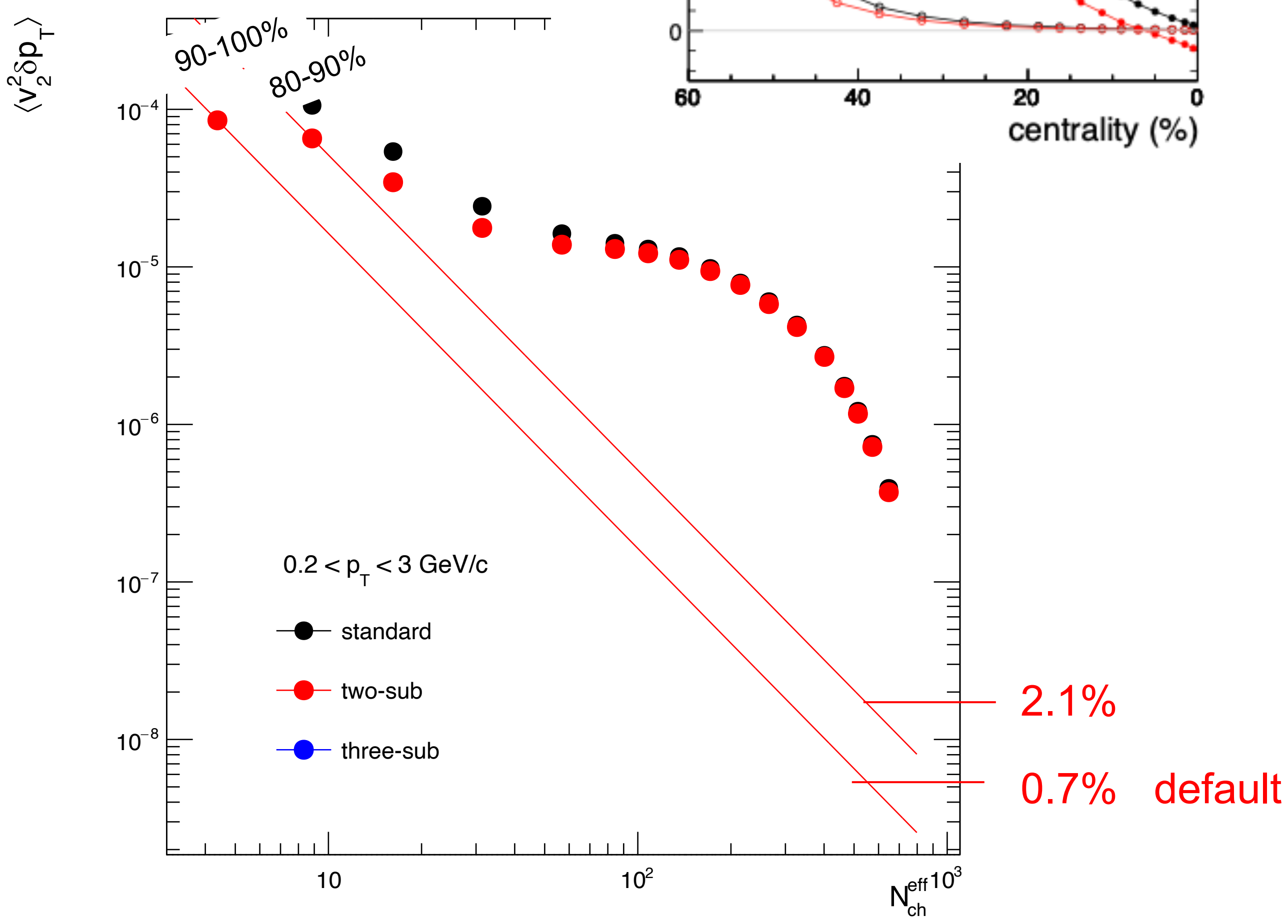

HIJING follow 1/N^2, expectation from independent source scenario. Jet quenching will reduce it.

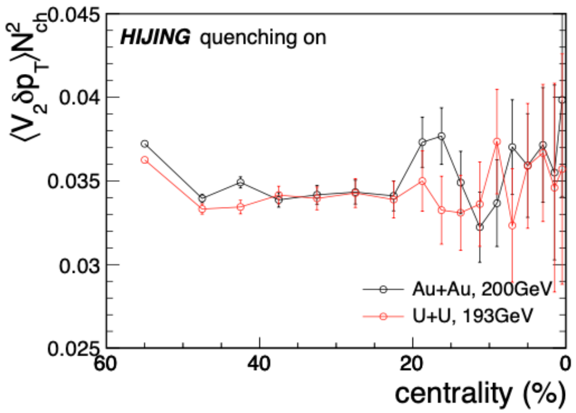

Lines extrapolation assuming $1/N^2$ scaling. Estimated non-flow contribution in 0-5% centrality is <0.5-2%.

Three-particle correlations are expected to be less sensitive to jet fragmentation and resonances

Nonflow would not affect the conclusions!

Section 3: Nuclear structure in isobaric ^{96}Ru and ^{96}Zr nuclei

$$\rho(r,\theta,\phi) = \frac{\rho_0}{1 + e^{(r - R(\theta,\phi))/a_0}}$$

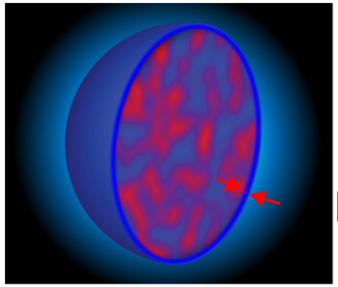

$$R(\theta,\phi) = R_0(1 + \beta_2[\cos\gamma Y_{2,0}(\theta,\phi) + \sin\gamma Y_{2,2}(\theta,\phi)] + \beta_3 Y_{3,0}(\theta,\phi))$$

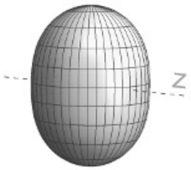

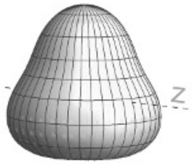

Lower energies experimental measurement

$$\beta_2 = \frac{4\pi}{3ZR_0^2}\sqrt{\frac{B(E2)\uparrow}{e^2}} \qquad \beta_3 = \frac{4\pi}{3ZR_0^3}\sqrt{\frac{B(E3)\uparrow}{e^2}}$$

	β_2	$E_{2_1^+}$ (MeV)	β_3	$E_{3_1^-}$ (MeV)
^{96}Ru	0.154	0.83	-	3.08
^{96}Zr	0.062	1.75	0.202,0.235,0.27	1.90

Evidence of static octupole moments at low energies is rather sparse.

Pear-shaped nuclei enable new-physics searches?

US Long Range Plan 2023

Sidebar 6.2 Radioisotope harvesting at FRIB for fundamental physics

The Facility for Rare Isotope Beams (FRIB) will yield the discovery of new, exotic isotopes and the measurement of reaction rates for nuclear astrophysics, and will produce radioactive isotopes that can be used for a broad range of applications, including medicine, biology, and fundamental physics.

Converting waste to wealth
Radioisotopes at FRIB are produced via fragmentation when accelerated ion beams interact with a thin target. Several isotopes, including those previously unobserved, across the entire periodic table will be produced in practical quantities for the first time in the water beam dump at the FRIB accelerator. The Isotope Harvesting Project provides a new opportunity to collect these isotopes, greatly enhancing their yield and real-time availability to enable a broad spectrum of research across multiple scientific disciplines. Isotopes will be extracted from the beam dump and chemically purified using radiochemistry techniques in a process called harvesting. Harvesting operates commensally, therefore providing additional opportunities for science.

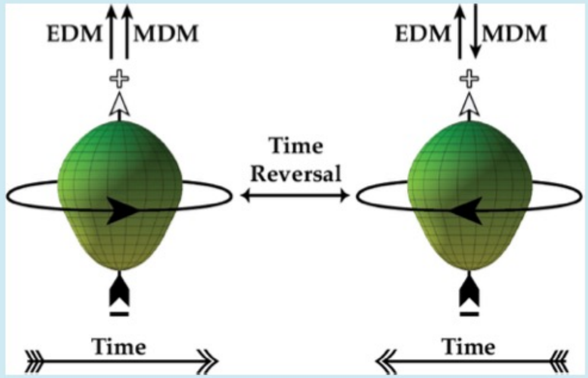

Figure 1. A pear-shaped nucleus spins counterclockwise or clockwise, depending on the direction of time. [S47]

Pear-shaped nuclei enable new-physics searches
With uranium-238 ion beams, these methods can produce heavy, pear-shaped nuclei that can be used to search for violations of fundamental symmetries that would signal new forces in nature. For example, a nonzero permanent electric dipole moment (EDM) would break parity and time-reversal symmetries. Figure 1 shows a pear-shaped nucleus spinning under applied electric and magnetic fields. Its magnetic dipole moment (MDM) is nonzero, and if its EDM is also nonzero, then its spin-precession rate changes if the direction of time is reversed. Heavy, pear-shaped nuclei can greatly amplify the sensitivity to a nonzero EDM and complement neutron EDM studies. Pear-shaped isotopes such as radium-225 and protactinium-229 will be produced in abundance at FRIB, and their EDM effects can be further enhanced by using them to form polar molecules, which can then be probed using cutting-edge laser techniques. The unique sensitivity of these experiments opens otherwise inaccessible windows on new physics.

P and *T* Violation in Nuclei

CP violation in the Standard Model is not enough for matter-antimatter asymmetry. Expect to find new physics responsible for it.

Searches for EDMs a very sensitive probes.
EDMs very small and difficult to measure.

Higher sensitivity via Schiff nuclear moments in heavy nuclei
-> octupole deformation enhancements

$$S_z = \frac{\langle e r^2 z\rangle}{10} - \frac{\langle r^2\rangle\langle e z\rangle}{6}$$

Schiff moments: constant electric field

CP-violating physics (unknown)

$$S \equiv \langle \Psi_0 | S_z | \Psi_0 \rangle = \sum_{k\neq 0} \frac{\langle \Psi_0 | S_z | \Psi_k \rangle \langle \Psi_k | V_{PT} | \Psi_0 \rangle}{E_0 - E_k} + \text{c.c.}$$

Nuclear deformation with large Schiff moments

Difference in nuclear energy

N. Auerbach et al., PRL76 4316(1996); J. Dobaczewski and J. Engel, PRL94, 232502(2005); T. E. Chupp et al., RevModPhys91, 015001(2019)

Unique isobar ^{96}Ru and ^{96}Zr Collisions

^{96}Ru+^{96}Ru and ^{96}Zr+^{96}Zr at $\sqrt{s_{NN}}$ =200 GeV

- A key question for any HI observable $\mathcal{O}$:

$$\frac{\mathcal{O}_{^{96}\mathrm{Ru}+^{96}\mathrm{Ru}}}{\mathcal{O}_{^{96}\mathrm{Zr}+^{96}\mathrm{Zr}}} \stackrel{?}{=} 1$$

- Expectation:

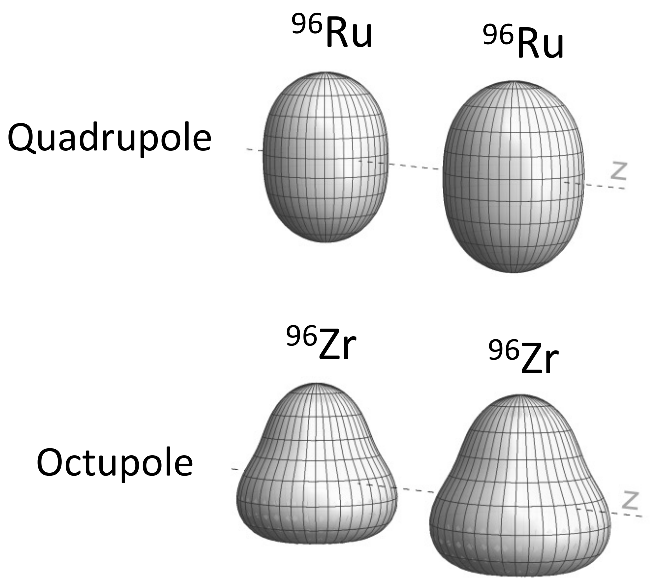

Deviation from 1 could have an origin in the nuclear structure, which impacts the initial state and then survives to the final state.

$$\mathcal{O} \approx b_0 + b_1\beta_2^2 + b_2\beta_3^2 + b_3(R_0 - R_{0,\mathrm{ref}}) + b_4(a - a_{\mathrm{ref}})$$

$$R_{\mathcal{O}} \equiv \frac{\mathcal{O}_{\mathrm{Ru}}}{\mathcal{O}_{\mathrm{Zr}}} \approx 1 + c_1\Delta\beta_2^2 + c_2\Delta\beta_3^2 + c_3\Delta R_0 + c_4\Delta a$$

Only probe structure differences

Species	β_2	β_3	a_0	R_0
Ru	0.162	0	0.46 fm	5.09 fm
Zr	0.06	0.20	0.52 fm	5.02 fm
difference	$\Delta\beta_2^2$	$\Delta\beta_3^2$	Δa_0	ΔR_0
	0.0226	-0.04	-0.06 fm	0.07 fm

Relate to neutron skin: $\Delta r_{\mathrm{np}} = \langle r_n \rangle^{1/2} - \langle r_p \rangle^{1/2}$

$$\Delta r_{np,\mathrm{Ru}} - \Delta r_{np,\mathrm{Zr}} \propto \underbrace{(R_0\Delta R_0 - \overbrace{R_{0p}\Delta R_{0p}) + 7/3\pi^2(a\Delta a}^{\text{charge}}}_{\text{mass}} - a_p\Delta a_p)$$

C. Zhang and J. Jia, PRL128, 022301(2022);
J. Jia and C. Zhang, PRC107, L021901(2023);
B. Bally et al., 2209.11042

Nuclear structure via v_n ratio

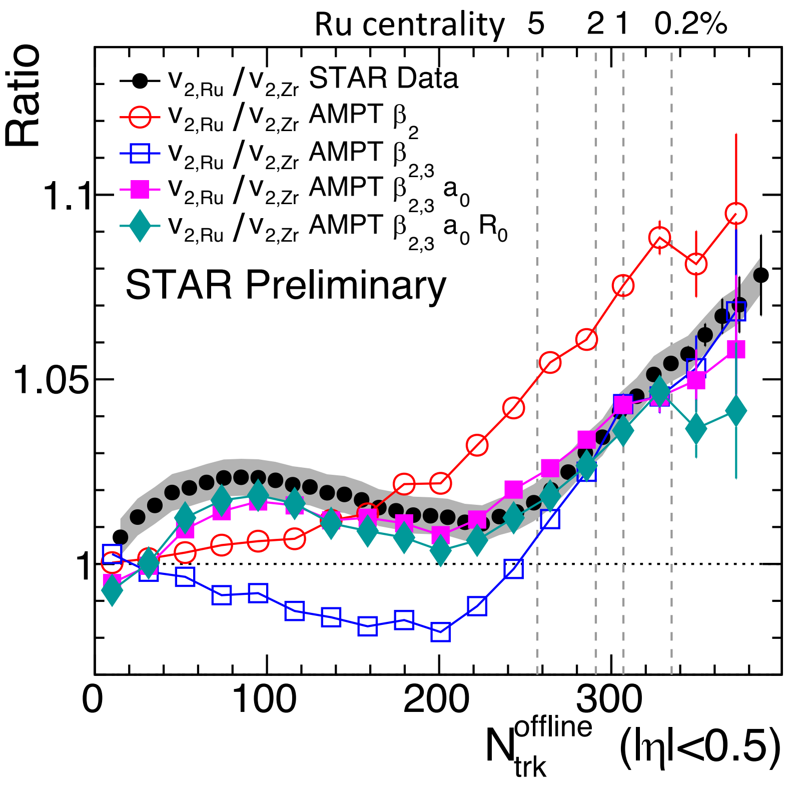

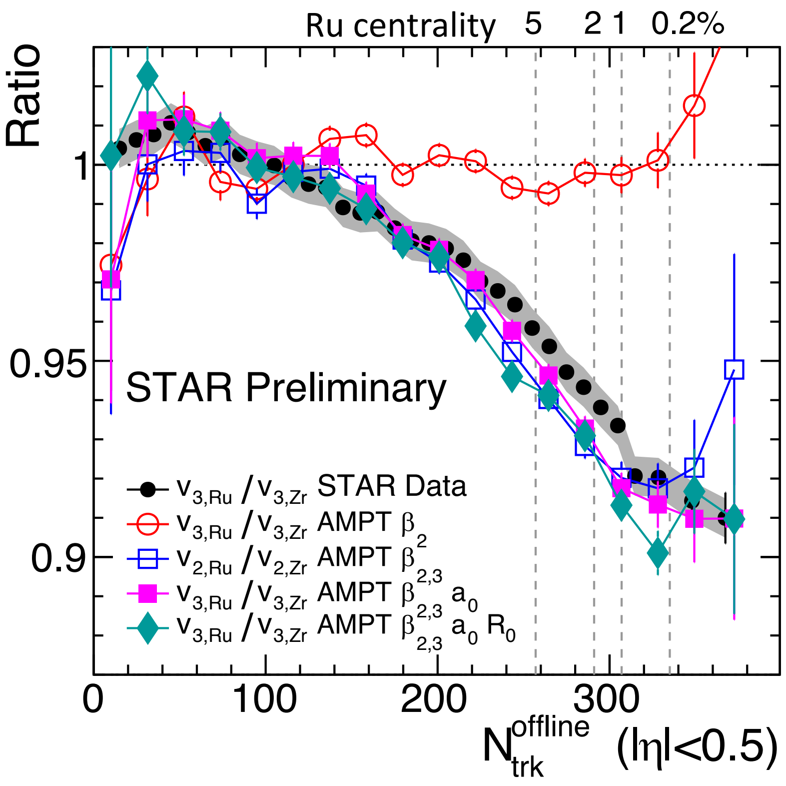

- β_{2Ru} ~ 0.16 increase v_2, no influence on v_3 ratio
- β_{3Zr} ~ 0.2 decrease v_2 in mid-central, decrease v_3 ratio
- Δa_0 = -0.06 fm increase v_2 mid-central, small impact on v_3
- Radius ΔR_0 = 0.07 fm only slightly affects v_2 and v_3 ratio.

- Direct observation of octupole deformation in ^{96}Zr nucleus
- Clearly imply the neutron skin difference between ^{96}Ru and ^{96}Zr
- Simultaneously constrain these parameters using different N_{ch} regions

Isobar ratios cancel final state effect

- Vary the shear viscosity by changing partonic cross-section
  - Flow signal change by 30-50%, the v_n ratio unchanged.

C. Zhang et al., PRC106, L031901(2022)

$$v_n = k_n \varepsilon_n$$

$$\frac{v_{n,\mathrm{Ru}}}{v_{n,\mathrm{Zr}}} \approx \frac{\varepsilon_{n,\mathrm{Ru}}}{\varepsilon_{n,\mathrm{Zr}}}$$

Robust probe of initial state!

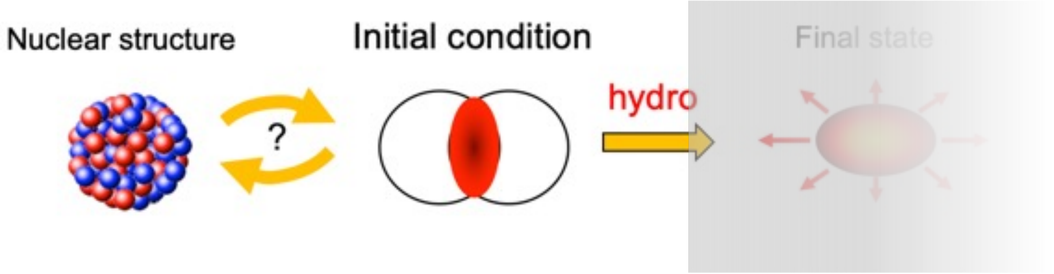

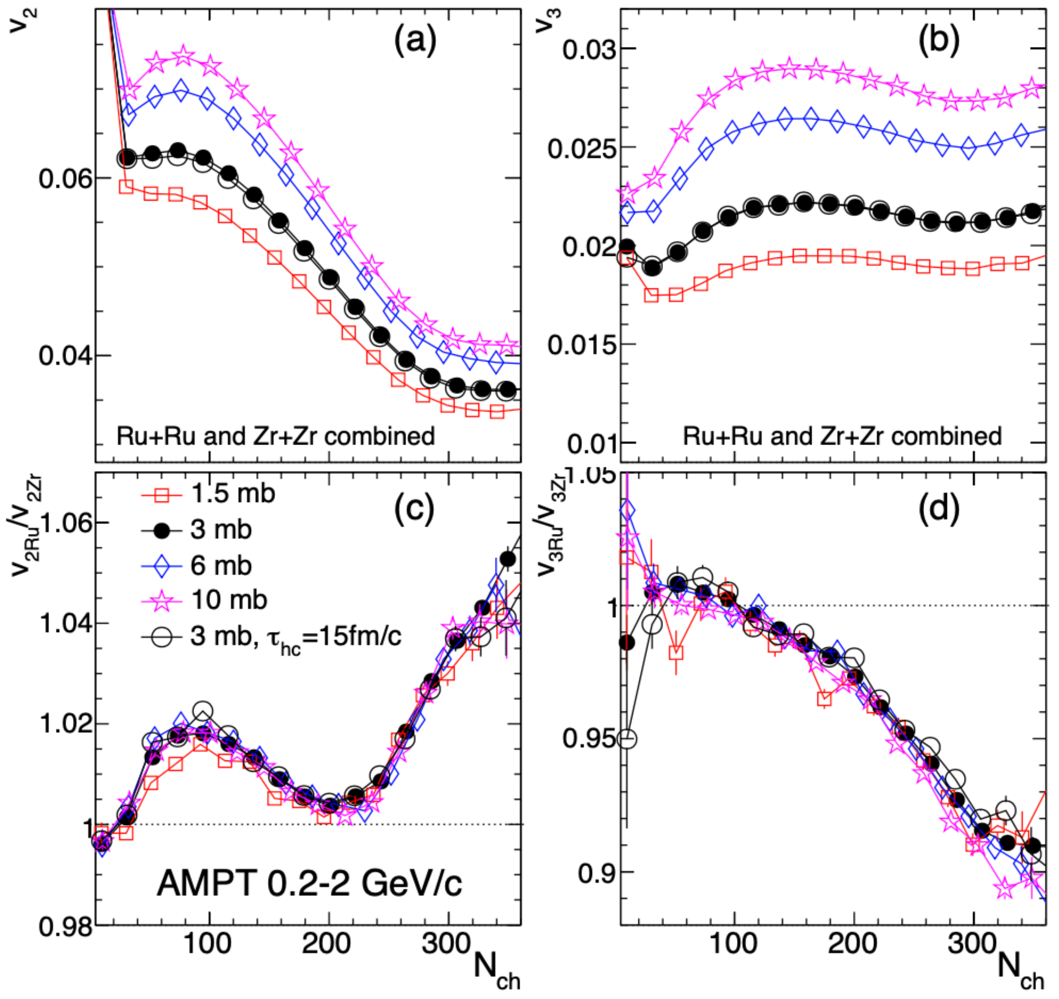

Nuclear structure influences everywhere

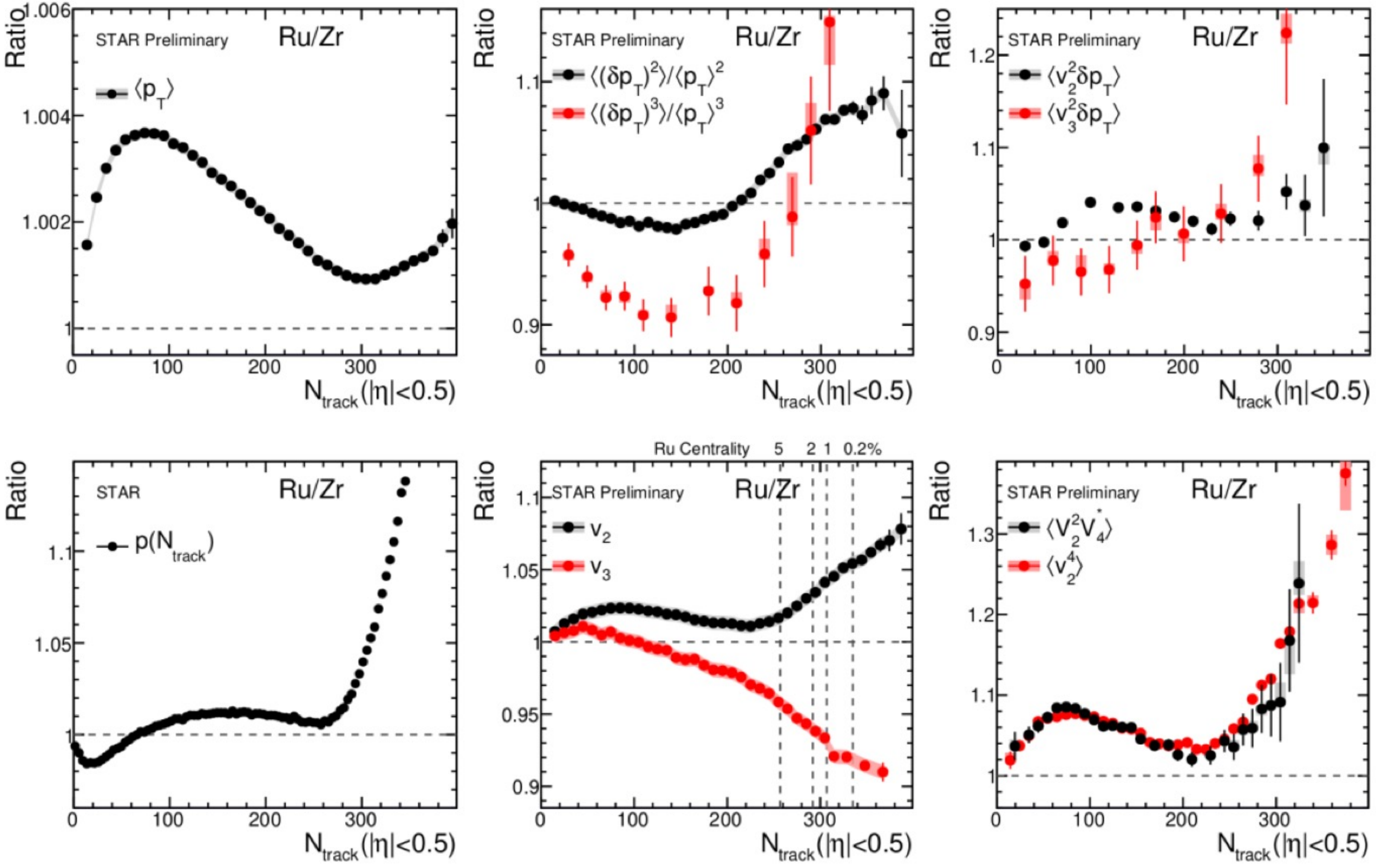

Signatures of the nuclear deformation at LHC

ATLAS, PRC107, 054910(2023)

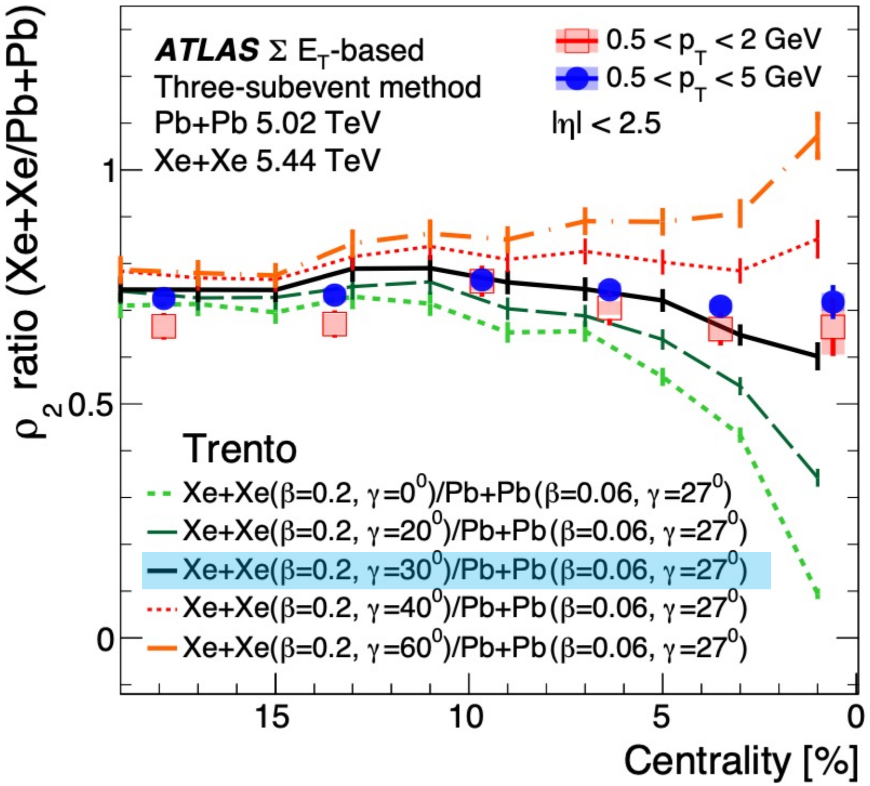

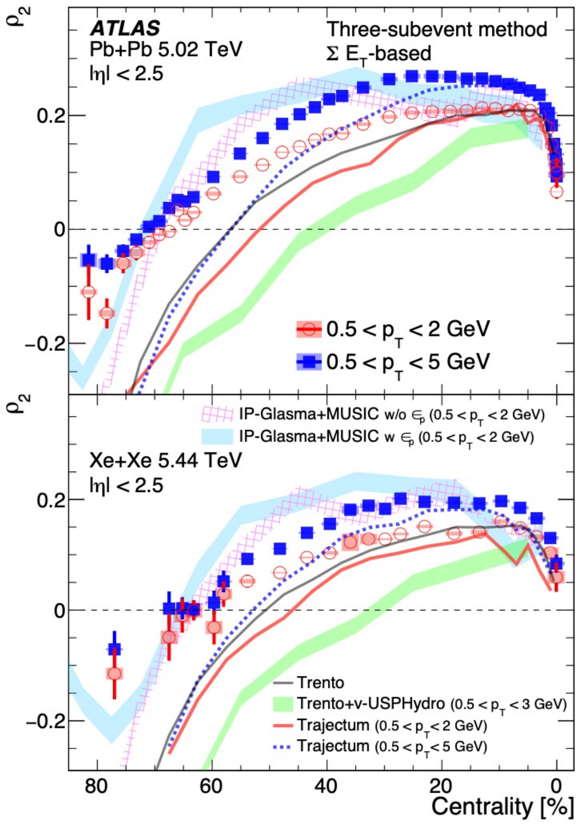

ALICE, PLB834, 137393(2022)

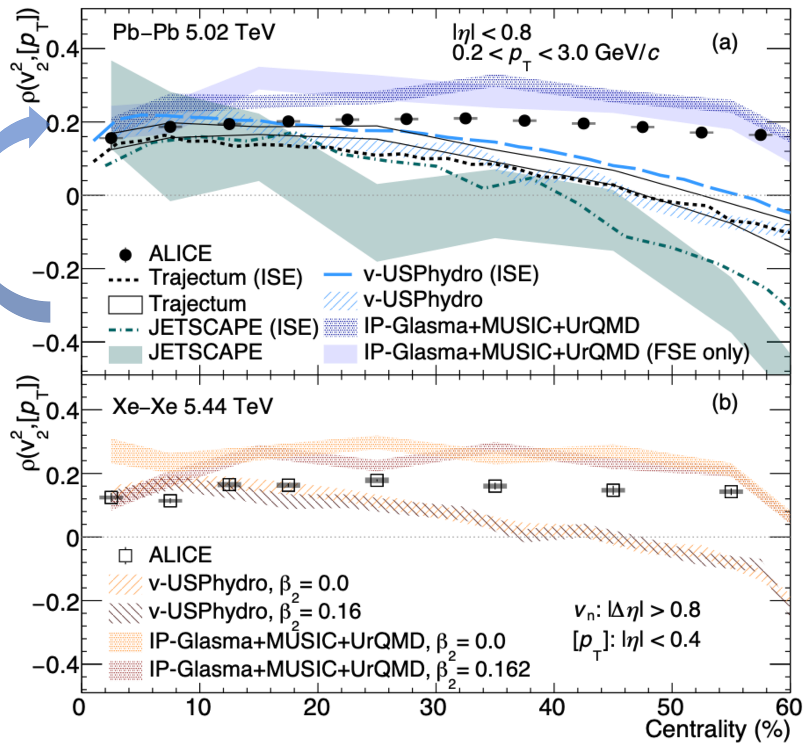

- The medium effect was mostly canceled.
- Study the triaxial shape of ^{129}Xe nuclei

Triaxiality fluctuation could wash out the difference between prolate and oblate. A. Dimri, S. Bhatta and J. Jia, EPJA59, 45(2023)

- Pave a novel way to characterize the initial state

Section 4: Nucleonic clustering in ^{16}O light nucleus

What is the origin of topological nucleonic clustering in the light nuclei?

US Long Range Plan 2023

Sidebar 4.3 Clusters in Nuclear Structure, Reactions, and Astrophysics

Light nuclei with even and equal numbers of protons and neutrons often exhibit cluster substructures when the energy sits near a threshold where parts of the nucleus would separate. The building blocks of these clusters are often alpha particles, or helium-4 nuclei. In nuclei with a few extra neutrons, molecular structures can form where the extra neutrons are shared between the alpha clusters. The second 0+ state of carbon-12 is called the Hoyle state (Fig 1) and is perhaps the most well-known and consequential alpha cluster state: without it, we wouldn't exist! The Hoyle state is crucial for the nucleosynthesis of carbon-12 and oxygen-16 in helium burning stars (Fig 2). In addition to low-background measurements of these reactions, oxygen-16 formation can be studied in terrestrial experiments by performing the reaction in reverse order, where a gamma-ray photon strikes the oxygen-16 and produces an alpha particle and carbon-12 (Fig 3). Clustering also plays an important role in the formation of alpha particles in the decay of heavy nuclei. Some alpha-emitting nuclei are useful for radiation therapy because the alpha particles travel only short distances in the human body and allow for the local targeting of cancer cells.

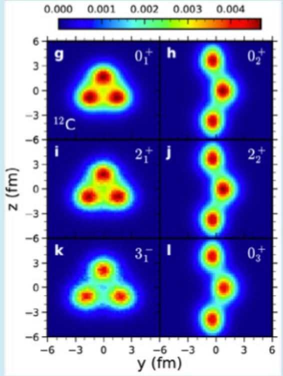

Figure 1. Various cluster structures calculated for nuclear states in the carbon-12 nucleus, using nuclear lattice effective field theory [S37].

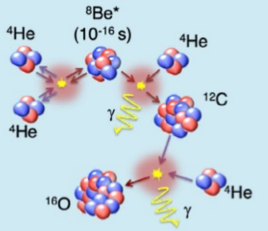

Figure 2. Schematic of the nuclear reactions involving alpha particles that power stars like the Sun. The structure of the helium-4 nucleus (alpha particle) is particularly conducive to clustering [S38].

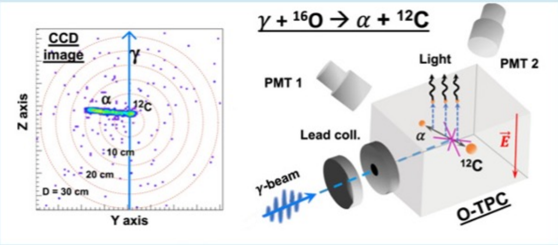

Figure 3. Demonstration of a novel measurement of the alpha capture reaction on carbon-12, using an optical time projection chamber and a gamma ray beam from the HIgS facility at TUNL. This reaction is highly influenced by resonances on alpha cluster states [S39].

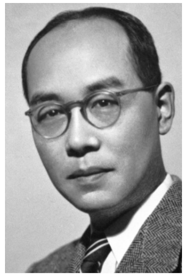

Hideki Yukawa

"for his prediction of the existence of mesons on the basis of theoretical work on nuclear forces"

1949

Run21 took the excellent dataset with iTPC and EPD:

Single-Beam Energy (GeV/nucleon)	$\sqrt{s_{NN}}$ (GeV)	Run Time	Species	Events (MinBias)
100	200	1 week	O+O	400 M 200 M (central)
100	200	1 week	d+Au	100M MB 100M Central

LHC: p+O and O+O collisions in 2025

${}^{16}_{8}$O with Woods-Saxon

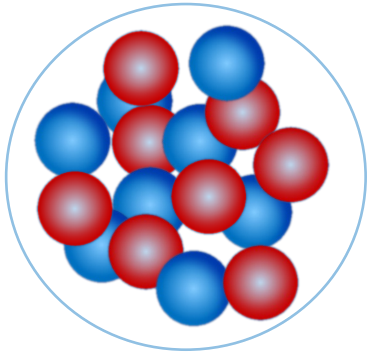

${}^{16}_{8}$O with α clusters

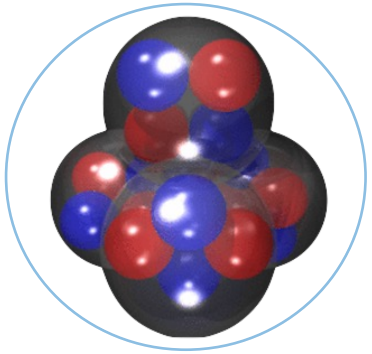

Many-nucleon correlations may also influence the fluctuation in eccentricity as $\varepsilon_n\{m\}$ in relativistic heavy-ion collisions?

Pioneer theory instructions of the nucleonic clustering

"Double magic number" in $^{16}_{8}O$ nuclei, possible alpha cluster inside based on the low energy.

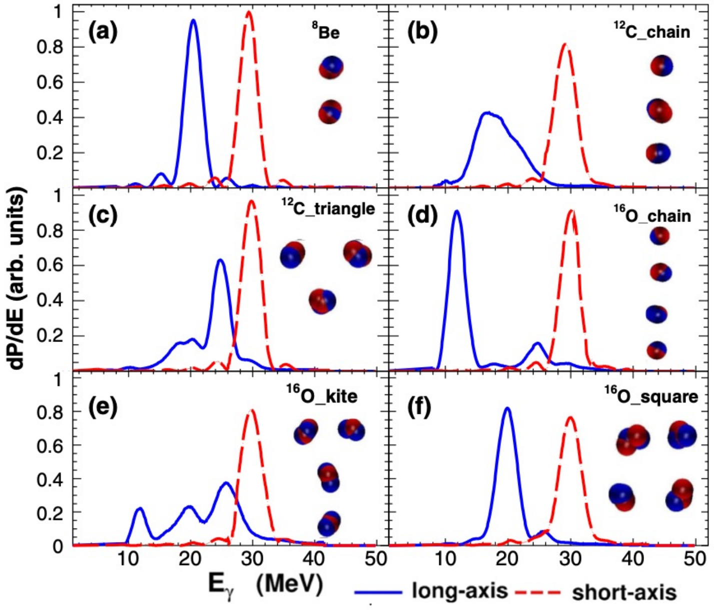

W. He, Y. Ma et al., PRL 113, 032605(2014)

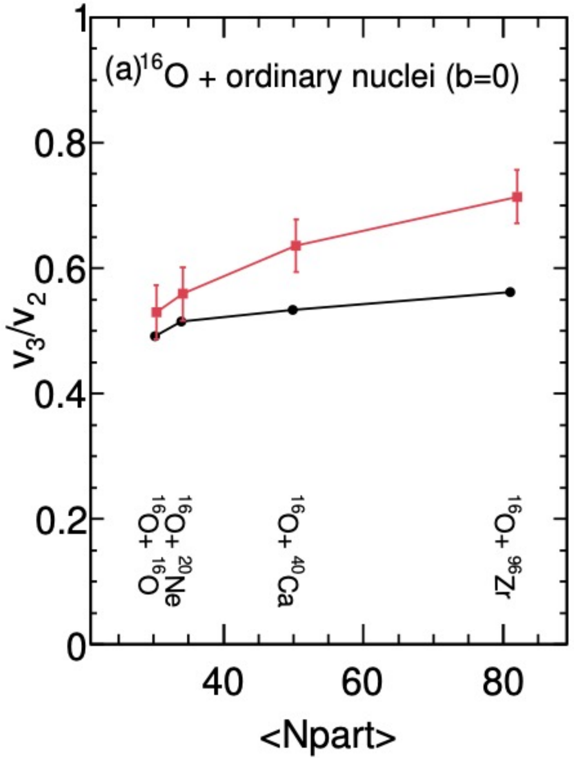

Y. Ma and S. Zhang, 2206.08218 (Handbook of Nuclear Physics)

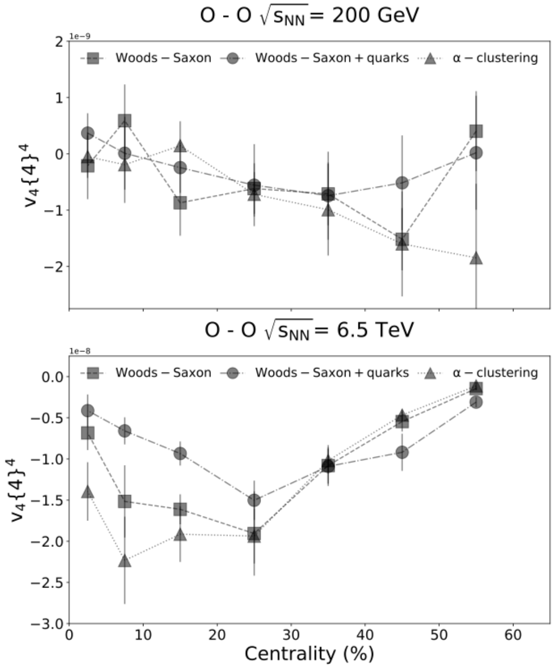

Nicholas et al., PRC104, L041901 (2021)

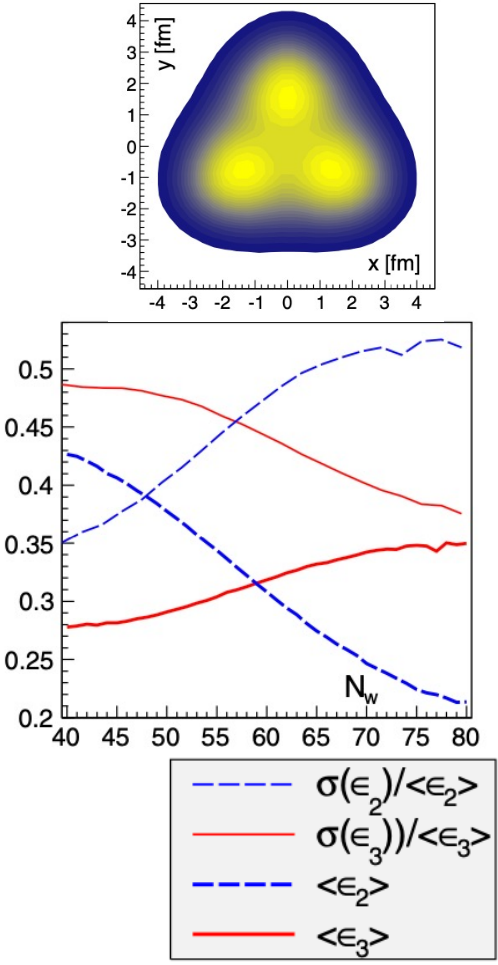

W. Broniowski and E. Arriola, PRL112, 112501(2014)

- ^{16}O nucleus could have different intrinsic topological structures.
- The initial configurations straightforwardly affect the final state observables in high energies.

Nucleon interactions in quantum many-body systems

***Woods-Saxon:** without many-body nuclear correlation*

***Nuclear Lattice Effective Field theory (NLEFT):** model with many-nucleon **correlation** including α clusters*

Lu et al., PLB797, 134863(2019)
M. Freer et al., RevModPhys90, 035004(2018)

Variational auxiliary field diffusion Monte Carlo (VMC):
MC solution of Schrödinger eq. from the time evolution of trial wave function.

Lonardoni et al., PRC97, 044318(2018)
J. Carlson and R. Schiavilla, RevModPhys70, 743(1998)

***ab-initio Projected Generator Coordinate Method (PGCM):** Wave function from variational calculation (as in density functional theory)*

Frosini et al., EPJA58, 62(2022); EPJA58, 63(2022); EPJA58, 64(2022)

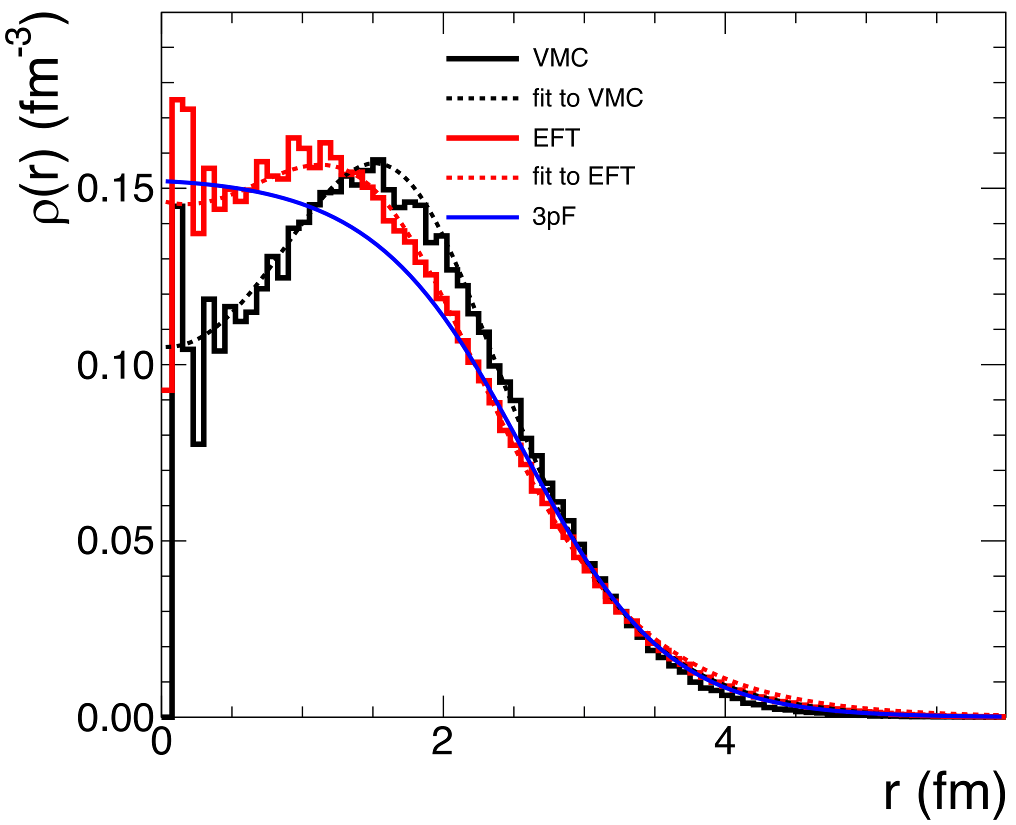

$v_2\{4\}/v_2\{2\}$: flow fluctuation in central O+O

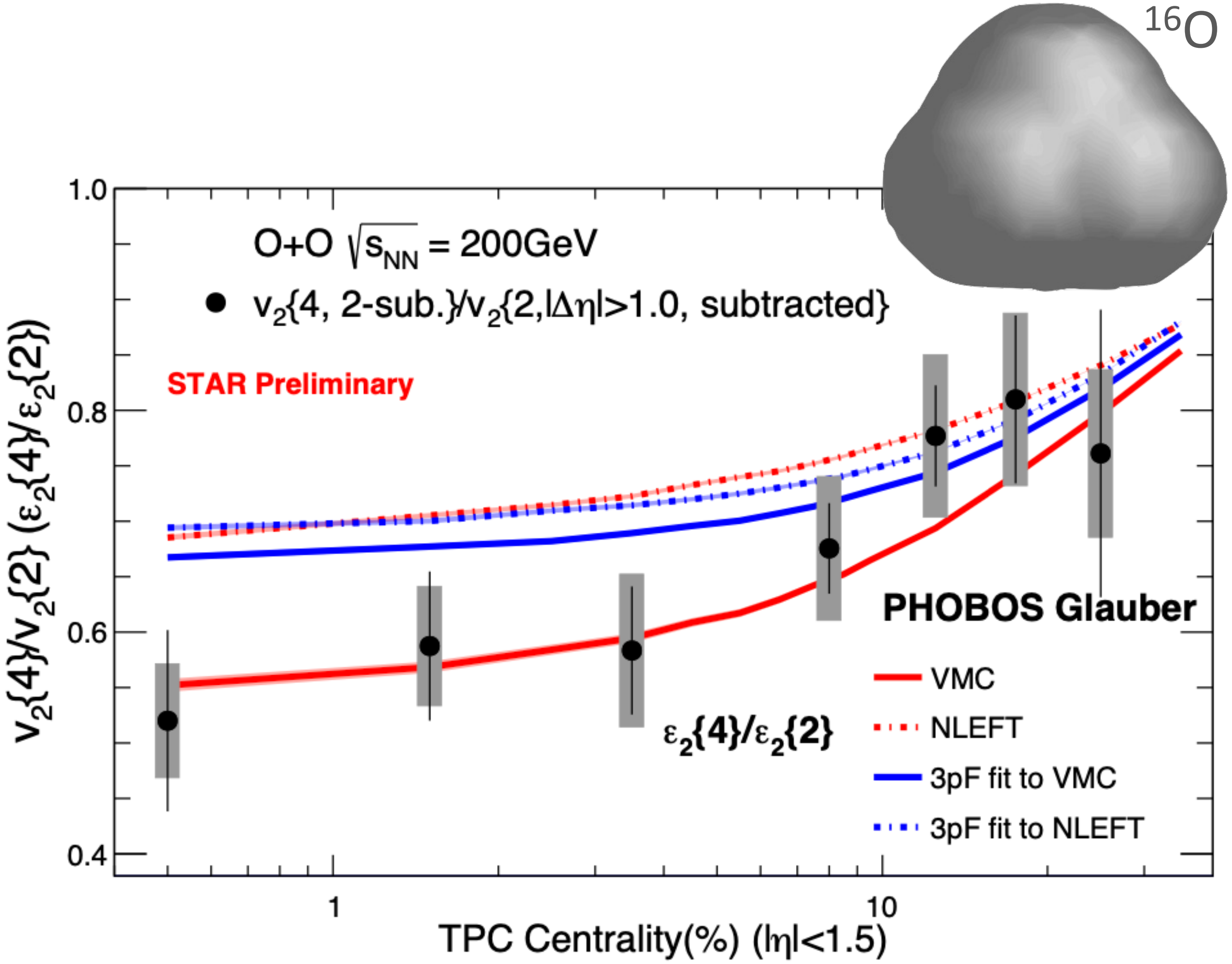

$\varepsilon_2\{4\}/\varepsilon_2\{2\}$ from three models:

1. WS is away from STAR data.

2. VMC and EFT have a visible difference.

Can many-nucleon correlations significantly impact the eccentricity fluctuations? However, these effects could be affected by sub-nucleon fluctuations.

STAR, PRL130, 242301(2023)

VMC and EFT theory have visible differences describing the $v_2\{4\}/v_2\{2\}$. The interplay between sub-nucleon fluctuation and many-nucleon correlation?

Detailed hydrodynamics and transport framework can elucidate the role of α cluster in light nuclei?

(more studies and checks are on the way)

Quark Glauber: PRC94, 024914(2016)
TRENTO: PRC92, 011901(2015) calculated by Giuliano Giacalone
Shengli Huang (STAR), arXiv:2312.12167

Section 5: Conclusions and Outlooks

1. The signatures of nuclear structure in heavy-ion collisions are everywhere, robust and reliable:

   Quadrupole, octupole deformations, and neutron skin thickness

2. Decoding the nuclear structure can be done via many tools:

   Bulk observables: flow $v_{n,}$ v_n-[p_T] correlations, N_{ch}, [p_T] and its fluctuations
   Ultra-peripheral collisions [in backup slides section 6]

3. The signals could be qualitatively described by the hydrodynamics and transport models:

   It helps us to understand further and better treat initial conditions theoretically.

4. Isobar collisions serve as the new and reliable tools to quantify nuclear structure:

   Final state effects are canceled by ratios.

5. O+O collisions potentially help to explore the intrinsic topological nucleonic clustering:

   It seems a very good potential to decipher the short-range interactions.

6. On the way to opening the interdisciplinary connection between low-energy and high-energy connections.

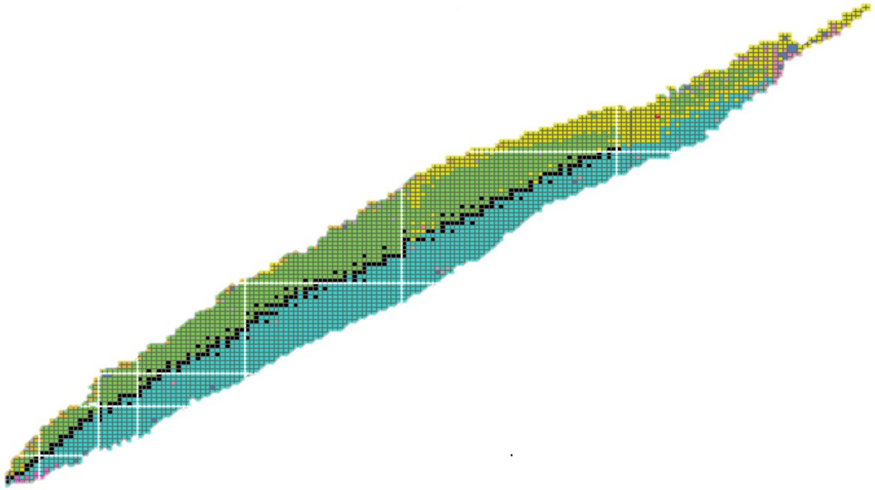

Nuclear deformation
Neutron skin
Nucleonic clustering
….

Nuclear deformation
Neutron skin
Nucleonic clustering
….

Low energy community

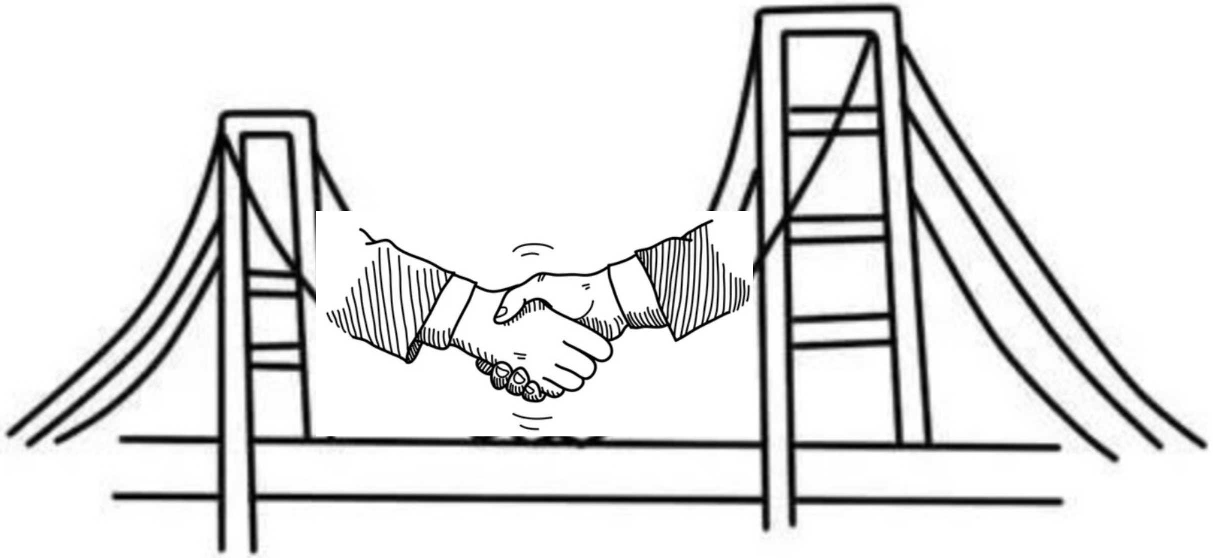

Heavy-ion community

Thank you

Section 6: Other ongoing endeavors and opportunities

(I apologize I may not have enough time to cover all the important results….)

Imaging the radial structures connected to symmetry energy

- Radial para. R_0, a_0 are properties of one-body distribution, can constrain via $\langle p_T \rangle$, $\langle N_{ch} \rangle$, and $v_{2RP} \sim v_2\{4\}$

More details in IS2023 Haojie Xu: https://indico.cern.ch/event/1043736/contributions/5363881/

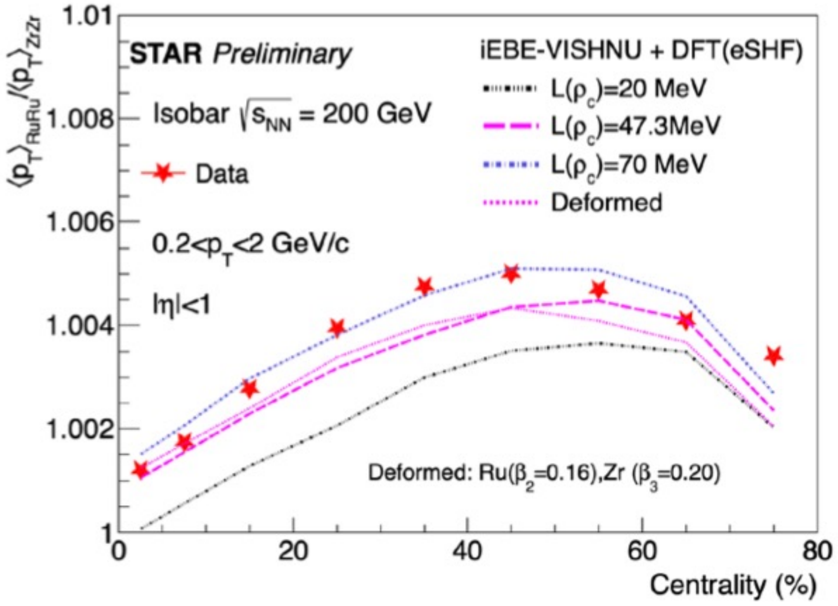

B. Li, et.al Universe 7, 182 (2021)

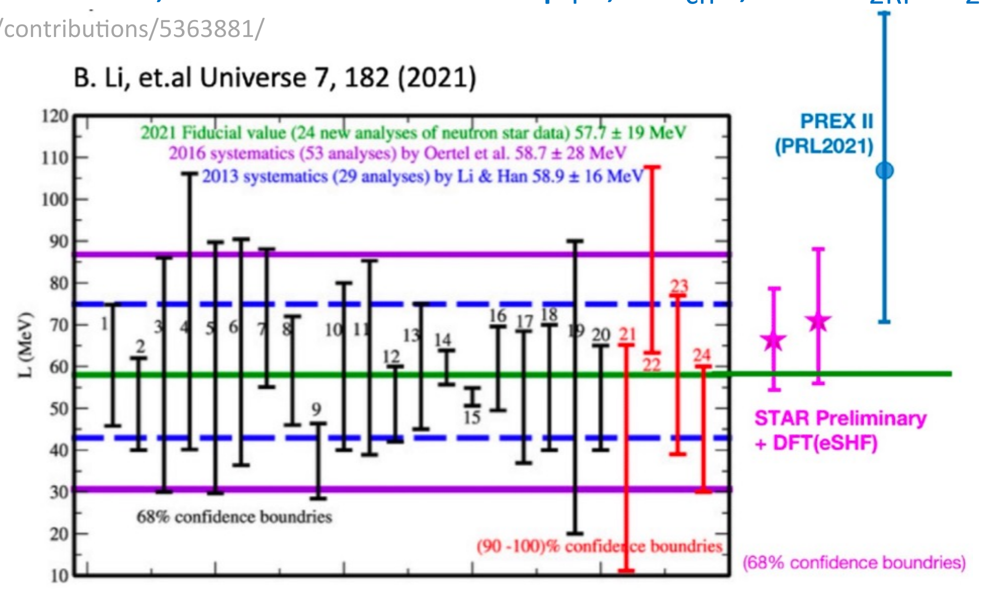

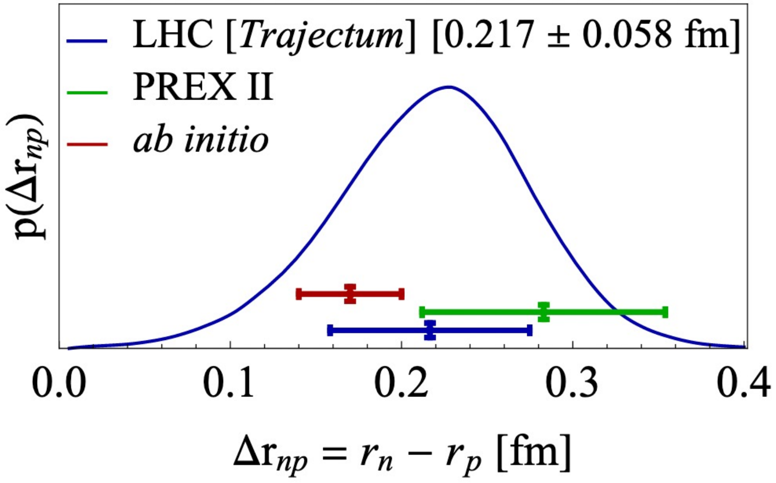

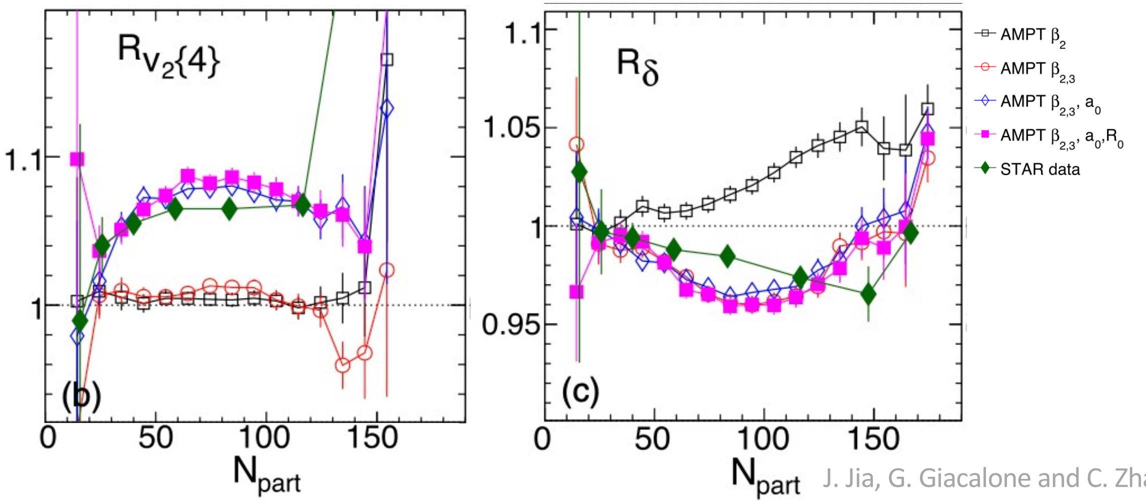

J. Jia, G. Giacalone and C. Zhang, PRL131, 022301(2023)

G. Giacalone, G. Nijs, and W. Schee, 2305.00015(PRL)

Heavy-ion collisions could assist in constraining symmetry energy.

Probing nuclear structure via photo-nuclear diffractive process in UPC

H. Mantysaari and B. Schenke, PRL117, 052301(2016);
H, Mantysaari, RepProgPhys83, 082201(2020)

Diffractive scattering amplitude

$$\mathcal{A}^{\gamma^* p \to V_p} \sim \int \mathrm{d}^2 b\, \mathrm{d}z\, \mathrm{d}^2 r \psi^{\gamma*}\Psi^V(r,z,Q^2)\mathbf{e}^{-\mathbf{ib}\cdot\Delta} N(r,x,b)$$

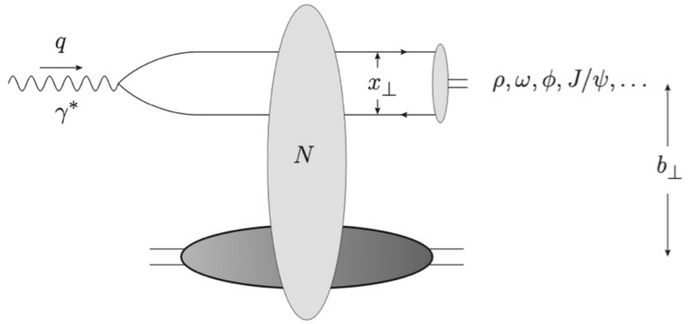

Impact parameter b, is the Fourier conjugate of the momentum transfer $\Delta \approx \sqrt{-t}$

$N(r,x,b)$ dipole-target scattering amplitude

H. Mantysaari, B. Schenke, C. Shen, and W. Zhao, PRL131, 062301(2023)

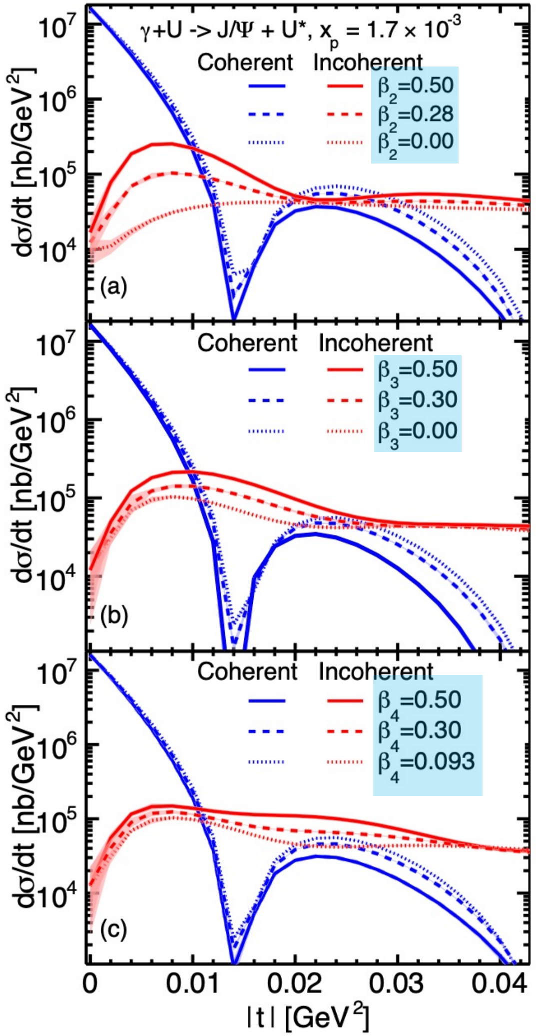

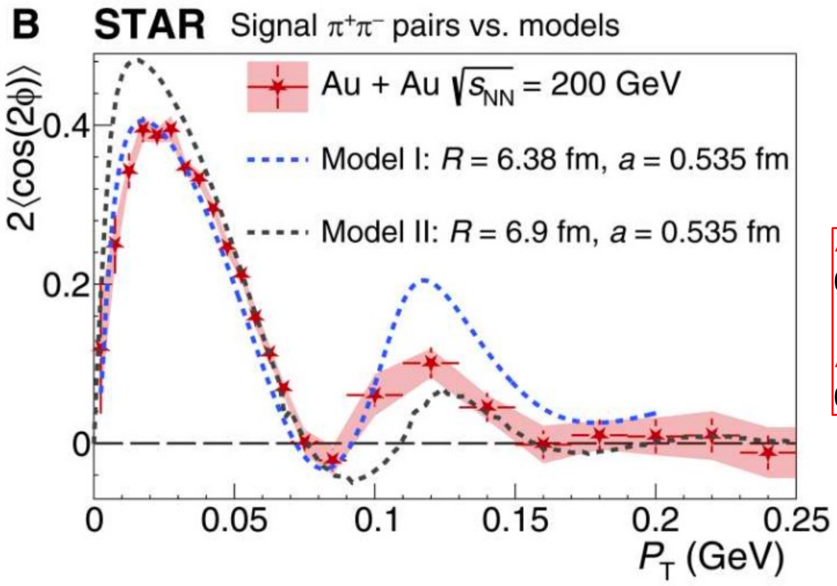

$\Delta R_{\mathrm{Au}} = R_n - R_p =$
0.17 ± 0.03 (stat.) ± 0.08 (sys.) fm

$\Delta R_{\mathrm{U}} = R_n - R_p =$
0.44 ± 0.05 (stat.) ± 0.08 (sys.) fm

STAR, Science Advance 9, 3903(2023)

β_2, β_3 and β_4 manifest themselves at different |t| regions (different length scales).

Possible understandings based on future Electron-Ion Collider

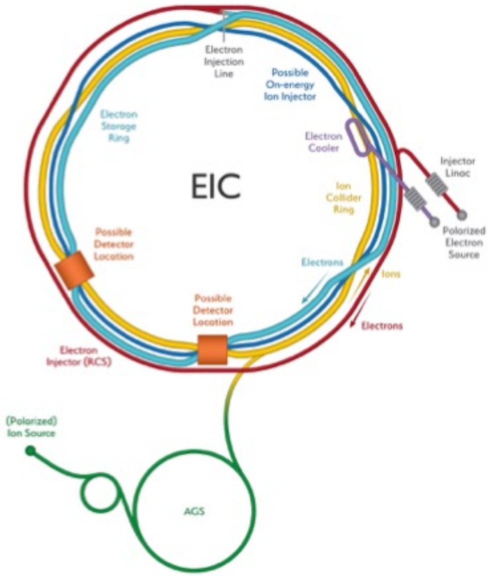

Nuclear structure (nucleon distributions) ? → 3D Gluon distributions

BeAGLE

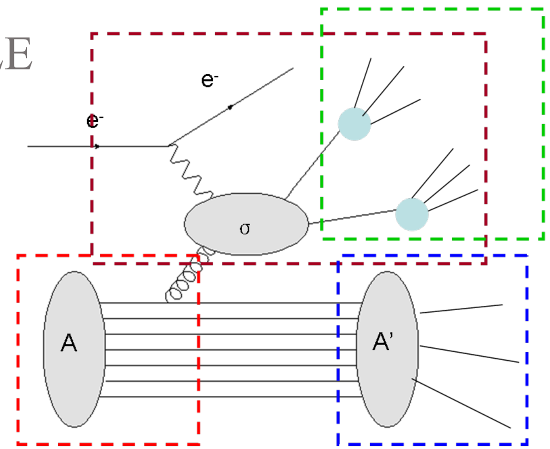

A hybrid model consisting of DPMJet and PYTHIA with nPDF EPS09.

Nuclear geometry by DPMJet and nPDF provided by EPS09.

Parton level interaction and jet fragmentation completed in PYTHIA.

Nuclear evaporation (gamma dexcitation/nuclear fission/fermi break up) treated by DPMJet

Energy loss effect from routine by Salgado&Wiedemann to simulate the nuclear fragmentation effect in cold nuclear matter

PRD106, 012007(2022)

Saturated gluonic matter (CGC) at Small x and moderate Q^2

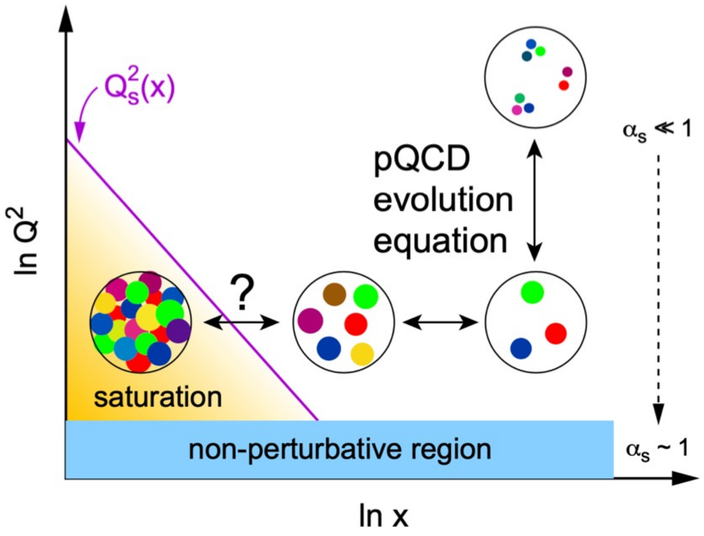

The nucleus A has an intrinsic nuclear structure.

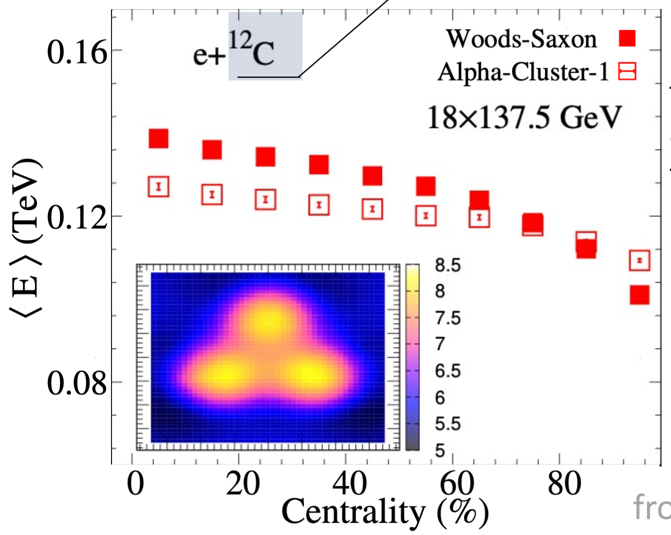

The system energy $\langle E \rangle$ measured in the forward detector is related to the impact parameter and the number of collisions.

The $\langle E \rangle$ in Forward detector acceptance is sensitive to nucleonic clustering in ^{12}C.

from Niseem Magdy

Low-energy spectroscopy vs high-energy snapshot method

- Intrinsic frame shape not directly visible in lab frame at time scale $\tau > I/\hbar \sim 10^{-21}s$

T. Nakatsukasa et al., RevModPhys88, 045004(2016)

- Mainly inferred from non-invasive spectroscopy methods.

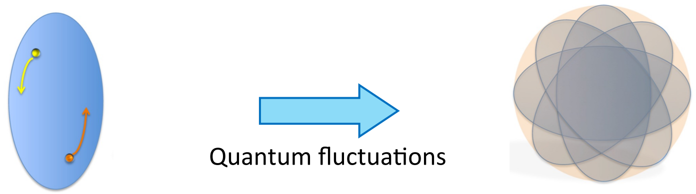

Correlated shape in intrinsic frame

Spherical shape in lab frame

Electron-scattering experiments

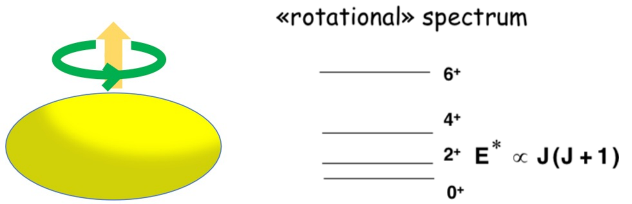

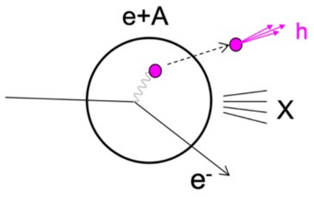

- Shape-frozen like snapshot in nuclear crossing (10^{-25}s << rotational time scale 10^{-21}s) probe entire mass distribution in the intrinsic frame via multi-point correlations.

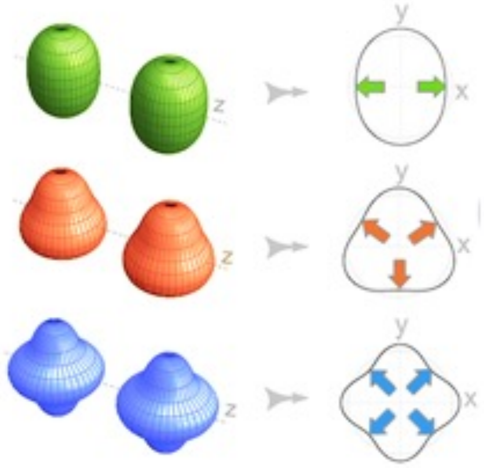

Collective flow-assisted imaging

Fast crossing

$\tau \approx 2R_0/\gamma \lesssim 0.1\mathrm{fm}/c$

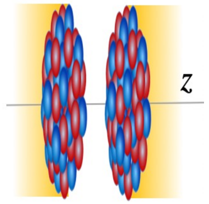

Large multiplicity

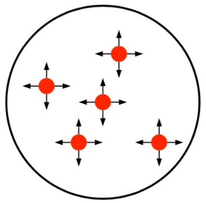

G. Giacalone et al., PRC100, 024905(2019)

$\mathbf{r} = re^{i\phi}$

Intrinsic frame

$$S(\mathbf{r}_1,\mathbf{r}_2) = \langle\rho(\mathbf{r}_1)\rho(\mathbf{r}_2)\rangle - \langle\rho(\mathbf{r}_1)\rangle\langle\rho(\mathbf{r}_2)\rangle$$

$$\epsilon_2 = \frac{\int_{\mathbf{r}} \mathbf{r}^2 S(\mathbf{r})}{\int_{\mathbf{r}} |\mathbf{r}|^2 \langle S(\mathbf{r})\rangle} \Rightarrow \langle\varepsilon_2^2\rangle = \frac{\int_{\mathbf{r}_1,\mathbf{r}_2} (\mathbf{r}_1)^2(\mathbf{r}_2^*)^2 S(\mathbf{r}_1,\mathbf{r}_2)}{\left(\int_{\mathbf{r}} |\mathbf{r}|^2\langle S(\mathbf{r})\rangle\right)^2}$$